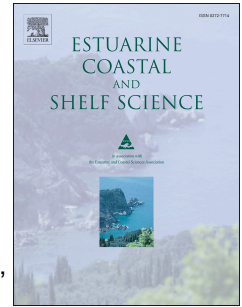


Accepted Manuscript

Structure of late summer phytoplankton community in the Firth of Lorn (Scotland) using microscopy and HPLC-CHEMTAX

Ana C. Brito, Carolina Sá, Carlos R. Mendes, Tim Brand, Ana M. Dias, Vanda Brotas, Keith Davidson



PII: S0272-7714(15)30015-9

DOI: [10.1016/j.ecss.2015.07.006](https://doi.org/10.1016/j.ecss.2015.07.006)

Reference: YECSS 4823

To appear in: *Estuarine, Coastal and Shelf Science*

Received Date: 5 November 2014

Revised Date: 19 June 2015

Accepted Date: 7 July 2015

Please cite this article as: Brito, A.C., Sá, C., Mendes, C.R., Brand, T., Dias, A.M., Brotas, V., Davidson, K., Structure of late summer phytoplankton community in the Firth of Lorn (Scotland) using microscopy and HPLC-CHEMTAX, *Estuarine, Coastal and Shelf Science* (2015), doi: 10.1016/j.ecss.2015.07.006.

This is a PDF file of an unedited manuscript that has been accepted for publication. As a service to our customers we are providing this early version of the manuscript. The manuscript will undergo copyediting, typesetting, and review of the resulting proof before it is published in its final form. Please note that during the production process errors may be discovered which could affect the content, and all legal disclaimers that apply to the journal pertain.

Structure of late summer phytoplankton community in the Firth of Lorn (Scotland) using microscopy and HPLC-CHEMTAX

Ana C. Brito^{1,*}, Carolina Sá¹, Carlos R. Mendes², Tim Brand³, Ana M. Dias¹, Vanda Brotas¹, Keith Davidson³

¹MARE-Marine and Environmental Sciences Centre, Faculdade de Ciências da Universidade de Lisboa, Campo Grande, 1749-016 Lisbon, Portugal

²Instituto de Oceanografia, Universidade Federal do Rio Grande (FURG), Av. Itália, Rio Grande, RS 96201-900, Brazil

³Scottish Association for Marine Science, Scottish Marine Institute, Oban, PA37 1QA, UK

Abstract:

The Firth of Lorn is at the mouth of one of Scotland's largest fjordic sea lochs, Loch Linnhe. This sea loch, which is fed by a number of other inner lochs, supplies a significant flow of freshwater, which frequently causes the stratification of the water column. To investigate how environmental conditions influence the spatial distribution of phytoplankton in this region water samples were collected for phytoplankton (pigments and microscopy), and other environmental variables including nutrients. Chemotaxonomy was used to estimate the contribution of different taxonomic groups to total chlorophyll *a* (phytoplankton biomass index). Good agreement was obtained between chemotaxonomy and microscopy data. The highest levels of chlorophyll *a* ($\sim 2.6 \text{ mg.m}^{-3}$) were found in the vicinity of Oban Bay, where cryptophytes, the most abundant group, dinoflagellates and other flagellates thrived in the stratified water column. Centric diatoms, mainly *Chaetoceros* sp. and *Skeletonema costatum*, were associated with NH_4 and SiO_2 concentrations and stratification, while pennate diatoms, mainly *Cylindrotheca* sp. and *Nitzschia* sp., were found to be associated with NO_3+NO_2 and high surface mixed layer depths. Four diatom groups were identified in accordance to their surface to volume ratios, as well as their affinity to environmental parameters (nutrients) and turbulence. This study used a combination of physico-chemical data, classical microscopy methods (appropriate for large cells $> 20\mu\text{m}$)

* Corresponding author. Email: acbrito@fc.ul.pt; Telephone: +351217500148; Fax: +351217500009

and HPLC-CHEMTAX approaches (for large and small cells) to evaluate the distribution of phytoplankton functional groups in a fjordic coastal area.

Keywords: Phytoplankton assemblage; Environmental drivers; HPLC-CHEMTAX; microscopy; Functional groups; Fjords.

1. Introduction

The Scottish west coast is characterised by the typical morphological, physical and hydrodynamic properties observed in other fjordic systems around the world. Sea lochs are narrow arms of sea with long, deep, steep-sided glacially carved basins that project into coastal land masses. They possess fjordic characteristics of a shallow sill that limits the horizontal exchange of water with the open ocean. Due to their large catchment areas, freshwater input to the coastal environment from fjords is commonly significant.

Fjords are typically characterised by a low salinity surface layer and dense deep water that may become isolated due to the presence of shallow sills. Deep water can be stagnant, mixing with surface water through diffusive vertical mixing during episodic renewal events (Austin and Inall, 2002). When wind conditions are favourable and freshwater input into the loch is low, flooding tidal saline water flows over the sill(s) and sinks to the bottom due to its higher density (Gade and Edwards, 1980; Geyer and Cannon, 1982). The pre-existing freshwater is lifted up and flushed away. If renewal events are not frequent, deep water will accumulate for several months or sometimes years and will have oxygen depletion and enhanced nutrient levels (e.g. Gade and Edwards, 1980; Edwards and Grantham, 1986).

The existence of aquaculture farms may emphasize bottom oxygen reduction and nutrient increase, if flushing is not recurrent. Nutrients in surface waters vary seasonally, peaking in the winter months, and decreasing post spring bloom (Lonborg et al. 2009, Fehling et al. 2006) following seasonal salinity stratification. While eutrophication symptoms have been occasionally reported in the past in some lochs (e.g. Edwards and Grantham 1986) and enhanced growth of macroalgae adjacent to aquaculture units can occur (Sanderson et al. 2012), there area is minimally anthropogenically impacted in terms of nutrient enrichment (Davidson et al. 2014).

Atlantic fjordic systems, such as the Scottish lochs are frequently subject to unstable weather conditions, given that wind strength and direction, precipitation and tides may vary substantially during short periods (Gaard et al., 2011). Such conditions may modify nutrient concentrations and have direct consequences in terms of phytoplankton biomass, leading to an increase or decrease in primary production due to rapid changes in oceanographic conditions (e.g. mixed layer depth, stratification). Changes in the stratification, light and turbulence conditions of the region may also have implications for community structure, favouring some phytoplankton groups over others (e.g. Margalef, 1978; Jones and Gowen, 1990), although these relationships are still poorly understood. Furthermore, tidal velocity and both wind intensity and direction may affect the structure and dynamics of the water column, which can determine the spatial pattern of phytoplankton distribution (Jones and Gowen, 1990).

Margalef's Mandala indicates that diatoms dominate in periods of high turbulence and nutrient concentrations (r-strategy) and dinoflagellates favouring more stratified and oligotrophic conditions (K-strategy; Margalef, 1978). This theory improved our understanding of phytoplankton dynamics. However, as discussed by Smayda and Reynolds (2001), the degree of vertical, micro-habitat structural differentiation that the turbulence axis allows, is also thought to be significant. There are several implications of this model compared to what has been previously proposed by Margalef (for details see Reynolds, 1988; 1996; 1997).

One of the innovations of Reynolds' approach is the identification of three primary adaptive strategies (C-S-R) rather than two (r-K). One of those strategies is characterised by small, r-selected, fast-growing, invasive, with high surface to volume ratio (S/V) colonist (C) species. These species are expected to dominate in stratified waters with high nutrient and light levels and would be susceptible to grazing (Alves-de-Souza et al., 2008). S species would be composed of large, with low S/V, slow-growing, K-selected, nutrient-stress tolerant organisms (Smayda and Reynolds, 2003). These species would dominate in high light, oligotrophic conditions and obtain their nutrients by mixotrophy or vertical migration (Alves-de-Souza et al., 2008). The R species would be the elongated but with high S/V ratio, light-harvesting, attuning, disturbance-tolerant ruderal species (Smayda and Reynolds, 2003). These species can harvest light under mixing conditions, with high nutrient concentrations (Alves-de-Souza et al., 2008).

Alvez-de-Sousa et al. (2008) presented one of the first applications of Reynolds' model to marine planktonic diatoms. They identified three diatom groups: D1, with $S/V > 1.5 \mu\text{m}^{-1}$ and composed of taxa such as *Pseudo-nitzschia*, *Cylindrotheca* and *Leptocylindrus* that were mainly correlated with nitrate; D2, with $S/V \sim 1 \mu\text{m}^{-1}$ and composed of several species of the genus *Chaetoceros*, also correlated with nitrate; and D3 with S/V between 0.5 and $0.8 \mu\text{m}^{-1}$ and composed of *Skeletonema*, *Talassionema* and *Rhizosolenia setigera* that were correlated with stratified conditions and high silicate concentrations.

In this study, we analysed phytoplankton data collected from the Firth of Lorn, in Western Scotland in order to: 1) evaluate the spatial distribution of the late summer phytoplankton community after a strong-wind event; 2) validate the chemotaxonomical approach to evaluate small phytoflagellates in this study region; 3) investigate the response of the phytoplankton community to physico-chemical parameters; and 4) provide insights regarding functional types in marine phytoplankton assemblages. Knowledge of how environmental conditions influence the spatial distribution of phytoplankton functional groups in sea-lochs is scarce. The phytoplankton community of the Firth of Lorn or adjacent sea lochs has been studied previously (Fehling et al. 2006 and references therein), however, these analyses typically concentrate on larger cells. Here, we combine the use of classical microscopy methods (appropriate for large cells) with novel HPLC-CHEMTAX approaches (for large and small cells) to evaluate the whole phytoplankton community. Environmental data were used to evaluate distribution of functional groups and to set the basis for future studies on phytoplankton temporal and spatial variability.

2. Methodology

2.1 Study Site

The Firth of Lorn, in western Scotland, is at the mouth of one of Scotland's largest fjordic sea lochs, Loch Linnhe (Figure 1). Loch Linnhe, which is fed by a number of other inner lochs, supplies a significant flow of freshwater to the coastal zone, which generally causes the stratification of the water column. The Firth of Lorn has a large variation in bathymetry and currents. Generally, net movement of seawater is northerly (Adams et al., 2014) and low salinity waters tend to run on the top of the water column due to their lower density. Tidal flows through the Sound of Luing and the Gulf of Corryvreckan, as well as its extension

westwards named Great Race, are important currents that are well documented (e.g. Dale et al., 2011). These flows may have a turbulent nature and contribute to the high dispersion of particles.

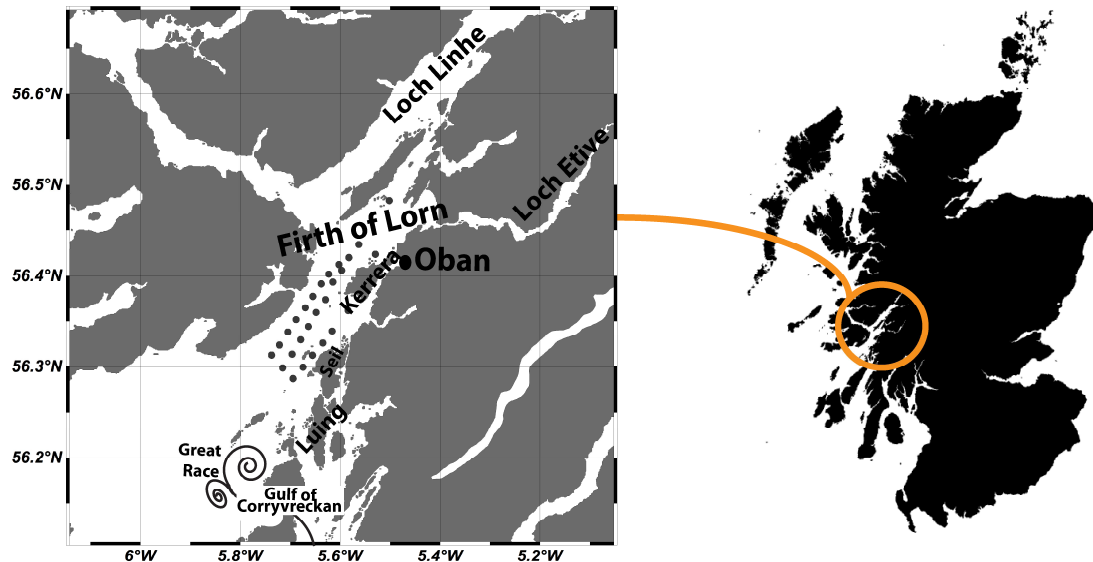


Figure 1 – Location of sampling station in the Firth of Lorn, Scotland's West coast. The location of the Great Race is also presented.

2.2 Field campaign and environmental data

In-situ sampling was performed between the 10th and the 12th of September 2012, after a 1-week event of strong winds, onboard the Research Vessel 'Seol Mara'. Samples were collected at 27 stations, mostly during flood and high tide, throughout the study site in the Firth of Lorn (Figure 1). In each transect, stations were ~ 2 km apart from each other, with some exceptions due to the geomorphology of the system. The vertical profile of the water column was analysed for salinity and temperature using a Seabird CTD (conductivity–temperature–depth) profiler. Photosynthetic Active Radiation (PAR) was also measured. The instrument was also equipped with an *in vivo* chlorophyll fluorescence sensor, which was used to guide the sampling procedure at each station, and an additional oxygen sensor. The fluorescence probe was later calibrated with HPLC data, determined in the laboratory. Surface measurements taken with the fluorescence sensor were discarded for calibration purposes. Surface water samples (0-5m in depth) were collected at all stations, using a Niskin bottle, for nutrients, phytoplankton pigments and microscopy. At selected stations samples from the Deep Chlorophyll Maximum (DCM) were also collected.

2.3 Physical parameters

Seawater potential density (kg.m^{-3}) was determined from temperature, salinity and pressure data collected by the CTD profiler in order to evaluate the water column physical structure (Brainerd and Gregg, 1995). The surface mixed layer (SML) depth was defined as the depth where density variations exceeded 0.05 kg.m^{-3} over a 1 m interval according to:

$$\Delta\sigma_{\theta} = \sigma_{\theta}(z) - \sigma_{\theta}(z_0);$$

where Z_0 is the surface depth ($\sim 2 \text{ m}$) and $\sigma_{\theta}(z) = \rho_{\theta}(z) - 1000 \text{ Kg.m}^{-3}$ is the density anomaly for calculated potential density (ρ_{θ}). Water column stability (E) was estimated using vertical density variations, as a function of the buoyancy or the Brunt-Väisälä frequency (N^2), which is determined by

$$N^2 = -\frac{g\partial\rho}{\rho\partial z} (\text{rad}^2\text{s}^{-2})$$

where g is gravity. Stability was then calculated following:

$$E = \frac{N^2}{g} (10^{-8} \text{ rad}^2\text{m}^{-1})$$

All variables were calculated according to the international thermodynamic equation of seawater (TEOS-10; IOC et al., 2010) using the toolbox functions GSW v3.04 for MATLAB.

2.4 Nutrients

One sample of 0.1 L seawater was collected at each sampling station. Samples were placed in a cool box, transported to the laboratory as soon as possible, and immediately frozen at $-20 \text{ }^{\circ}\text{C}$. Nutrient analyses were performed on each sample in triplicate, using a Lachat 8500 Flow Injection Analysis (FIA) autoanalyser (Hach Lange) following the manufacture's methods (ammonium, Liao, 2008; phosphate, Egan, 2008; silicate, Diamond, 2003; nitrate+nitrite, Diamond, 2008) which are based on established wet chemical reaction followed by spectrophotometric detection (Grasshoff 1976). Calibration standards were adjusted to suit the concentration range of the samples and matrix matched with the samples using low nutrient seawater (35 psu) (supplied by OSIL UK). Analytical precision based on triplicate analyses for all nutrients is better than 95%, accuracy determined by

running an independent standard (OSIL UK) is better than 95% and limits of analytical detection better than 0.05 μM .

2.5 *Phytoplankton data*

2.5.1 HPLC pigment analysis

Water samples (1 L) were filtered in dim light onto Whatman GF/F filters (nominal pore size of 0.7 μm and 25 mm diameter) using vacuum pressure <5 in. Hg and immediately frozen for later HPLC pigment analysis. Samples were analysed in the 'Laboratory of Phytoplankton and Marine Microorganisms' at Federal University of Rio Grande, Brazil. The filters were placed in a screw-cap centrifuge tube with 3 mL of 95% cold-buffered methanol (2% ammonium acetate) containing 0.05 mg L⁻¹ trans- β -apo-8'-carotenal (Fluka) as internal standard. The samples were sonicated for 5 min in an ice-water bath, placed at -20°C for 1h, and then centrifuged at 1100 g for 5 min at 3 °C. The supernatants were filtered through Fluoropore PTFE membrane filters (0.2 μm pore size), to rid the extract from remains of filter and cell debris. Immediately prior to injection, 1000 μL of sample was mixed with 400 μL of Milli-Q water in 2.0 ml amber glass sample vials, and vials were placed in the HPLC cooling rack (4 °C). Methods for HPLC analyses (using a monomeric C8 column with a pyridine-containing mobile phase) are fully described in Zapata et al. (2000). The detection limit and quantification procedure of this method followed Mendes et al. (2007). Pigments were identified from both absorbance spectra and signal retention times in the photodiode array detector (SPD-M20A) or fluorescence detector (RF-10AXL; Ex. 430 nm/Em. 670 nm). Peaks were integrated using LC-Solution software, but all peak integrations were checked manually and corrected where necessary. The HPLC system was previously calibrated with pigment standards from DHI (Institute for Water and Environment, Denmark). For correction losses and volume changes, the concentrations of the pigments were normalized to the internal standard. Table 1 lists all pigments considered in this study and which were detected above the limit of quantification, along with the respective abbreviations.

2.5.2 CHEMTAX

The relative abundance of microalgal groups contributing to total chlorophyll *a* biomass was calculated from pigment concentration data using version 1.95 of CHEMTAX chemical

taxonomy software (Mackey et al., 1996; Wright et al., 1996, 2009). CHEMTAX uses a factor analysis and steepest-descent algorithm to find the best fit of the data on to an initial pigment ratio matrix. Calculations methods and procedures are fully described in Mackey et al. (1996).

Based on the identified diagnostic pigments and confirmation of the higher taxonomic groups by microscopic analysis, seven algal groups were loaded on CHEMTAX: diatoms-1 (with chlorophyll c_1), dinoflagellates-1 (peridinin-containing dinoflagellates), cryptophytes, prasinophytes (with prasinoxanthin), haptophytes-6 (e.g. *Emiliana huxleyi*), haptophytes-7 (e.g. *Chrysochromulina* spp.) and haptophytes-8 (e.g. *Phaeocystis* spp.). The loaded pigments were Chl c_3 , Chl c_1 , Perid, But-fuco, Fuco, Neo, Hex-kfuco, Viola, Prasino, Hex-fuco, Dino, Zea, Lut, Chl b , Allo, Chl c_2 -MGDG [18:14], Chl c_2 -MGDG [14:14] and Chl a (see Table 2). The initial pigment ratios of prasinophytes-3, cryptophytes, haptophytes-7 and haptophytes-8 were obtained from literature (Higgins et al., 2011). For diatoms-1, dinoflagellates-1 and haptophytes-6 the pigment ratios were calculated using the mean values obtained from single cultures obtained by the authors from the Culture Collection of Algae and Protozoa (CCAP) (<http://www.sams.ac.uk/ccap>). The following species were considered: 1) the diatoms (type 1) *Amphora coffeaeformis*, *Bellerochea malleus*, *Ditylum brightwellii*, *Extubocellulus cribiger*, *Odontella aurita*, *Phaeodactylum tricornutum*, *Skeletonema costatum* and *Thalassiosira pseudonana*; 2) the dinoflagellates (type 1) *Alexandrium minutum*, *Alexandrium tamarense*, *Amphidinium carterae*, *Lingulodinium polyedrum*, *Prorocentrum micans*, *Prorocentrum minimum*, *Pyrocystis lunula* and *Scrippsiella trochoidea*; and 3) the haptophyte (type 6) *Emiliana huxleyi*.

Chlorophytes were not included in the CHEMTAX analysis as significant positive correlations ($R^2 > 0.8$; $p < 0.01$) were found between prasinoxanthin (exclusive of prasinophytes) and concentrations of chlorophyll b , lutein, zeaxanthin and violaxanthin (pigments present in chlorophytes and prasinophytes), hence the observed chlorophyll b concentrations were attributed to prasinophytes. The inclusion of three types of haptophytes in the input matrix was based on the detected pigments and on the high complexity of haptophytes, which have eight subgroups with different pigment profiles (Zapata et al., 2004).

The CHEMTAX analysis followed the procedure adopted by Wright et al. (2009). A series of 60 pigment ratios matrices were generated by multiplying each ratio from the initial matrix by a random function to optimize the matrix. The average of the best six output matrices

(with the lowest residual or root mean square error) were taken as the optimized results. The initial and final ratios are given in Table 2. In order to account for pigment ratios' variation with irradiance and/or nutrient availability, the data for each station were broken down into 2 bins (surface and DCM). The output data are presented as absolute concentrations ($\text{mg}\cdot\text{m}^{-3}$) of chlorophyll *a* attributed to each phytoplankton group.

2.5.3 Microscopy

Samples were collected in 125 ml bottles at the same stations and depths as described for HPLC analysis and preserved using neutral lugol solution. For analysis, samples were carefully agitated in order to obtain a reasonable homogenization of the solution. Sedimentation was carried out using 100 ml chambers for 48 hours. Quantification was conducted in an inverted microscope according to Lund *et al.* (1958) and Utermöhl (1958). Species identification followed Chrétiennot-dinet (1990), Hoppenrath (2009), Ricard (1987), Sournia (1986) and Tomas (1997).

2.6 Statistical analyses

In order to explore the relationships between the phytoplankton data and environmental conditions, a Canonical Correspondence Analysis (CCA) was performed in the CANOCO 4.5 software, similar to Fehling *et al.* (2012). The statistical significance was evaluated through a Monte Carlo permutation test. This analysis is effective in revealing the relationships between the spatial and temporal structure of communities and the environmental factors that might be responsible. Regression analyses were also used to evaluate the agreement between phytoplankton cell abundances and CHEMTAX results.

3. Results

3.1 Oceanographic conditions

Generally, at the time of sampling, the water column was mixed, with salinities higher than 32 psu, except in the most inner stations, i.e. the ones with the strongest freshwater influence. In the most inner stations there was a slight stratification and surface salinities were down to 24 psu due to the influence of the freshwater flow. In general terms, salinities

were always higher in the bottom layers of the water column. Higher temperatures were also found in the bottom layers of the water column, except in the station that directly receives water from the Loch Linnhe that had elevated temperatures in the top layers. A peak in chlorophyll *a* was recorded in the surface waters (0 to 10m) of the most inner stations. An oxygen peak was observed at the stations with the highest chlorophyll *a* concentrations. An oxygen minimum located at the subsurface waters (between 1 and 3 m) of the most inner station was observed. The PAR decay through the water column is stronger in the most inner stations. Interestingly, the PAR decay also seems to be slightly stronger in the most offshore stations, i.e. in the ones closest to the open sea (Figure 2).

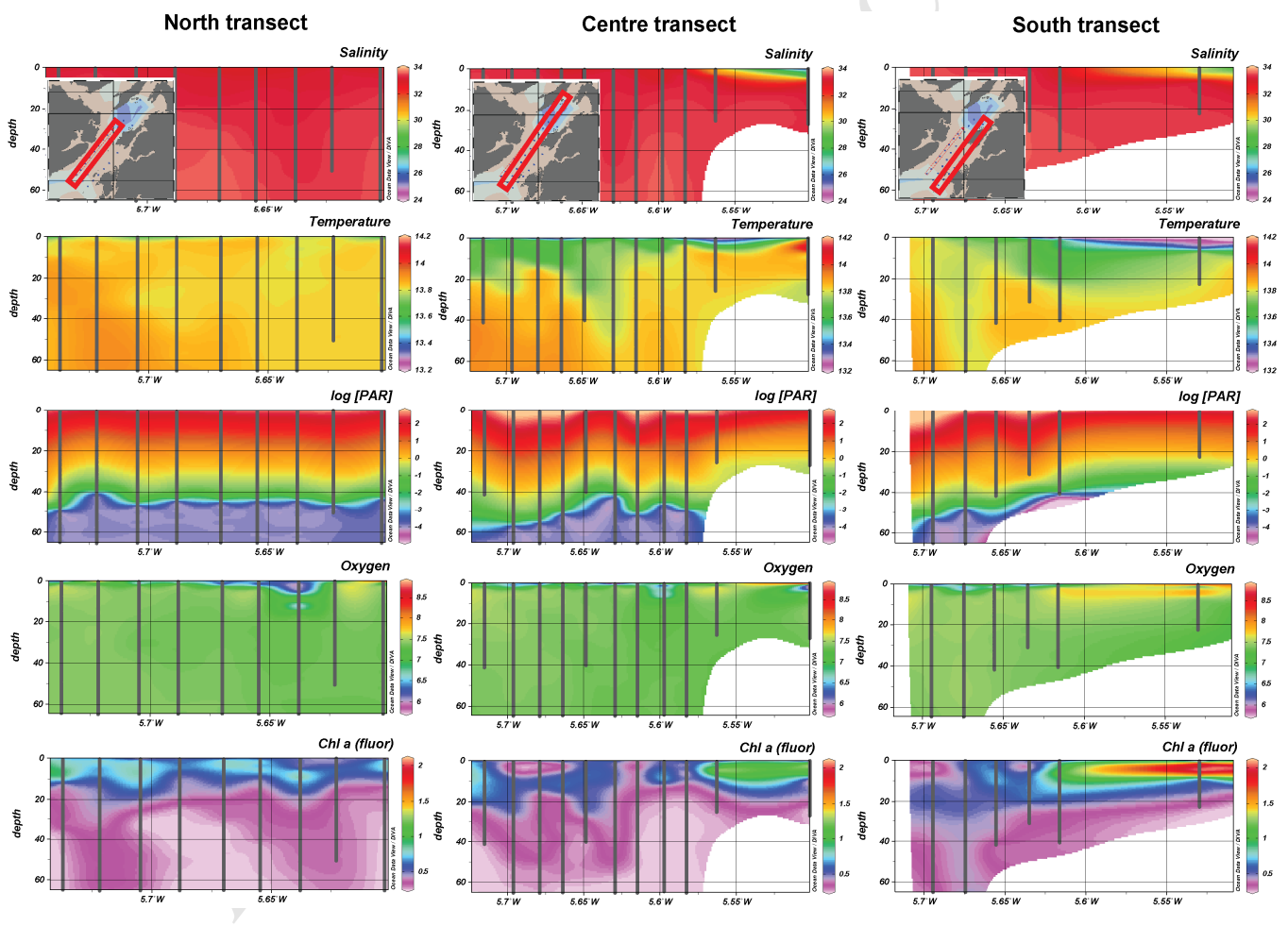


Figure 2 – Vertical profiles of salinity, temperature ($^{\circ}\text{C}$), chlorophyll *a* ($\text{mg}\cdot\text{m}^{-3}$), oxygen ($\text{mg}\cdot\text{L}^{-1}$) and $\log(\text{PAR})$ measurements taken by CTD (and additional sensors) in the Firth of Lorn. Results are presented with contours to enhance clarity. Note that chlorophyll *a* concentrations obtained by profiling fluorometer were calibrated with in-situ HPLC measurements.

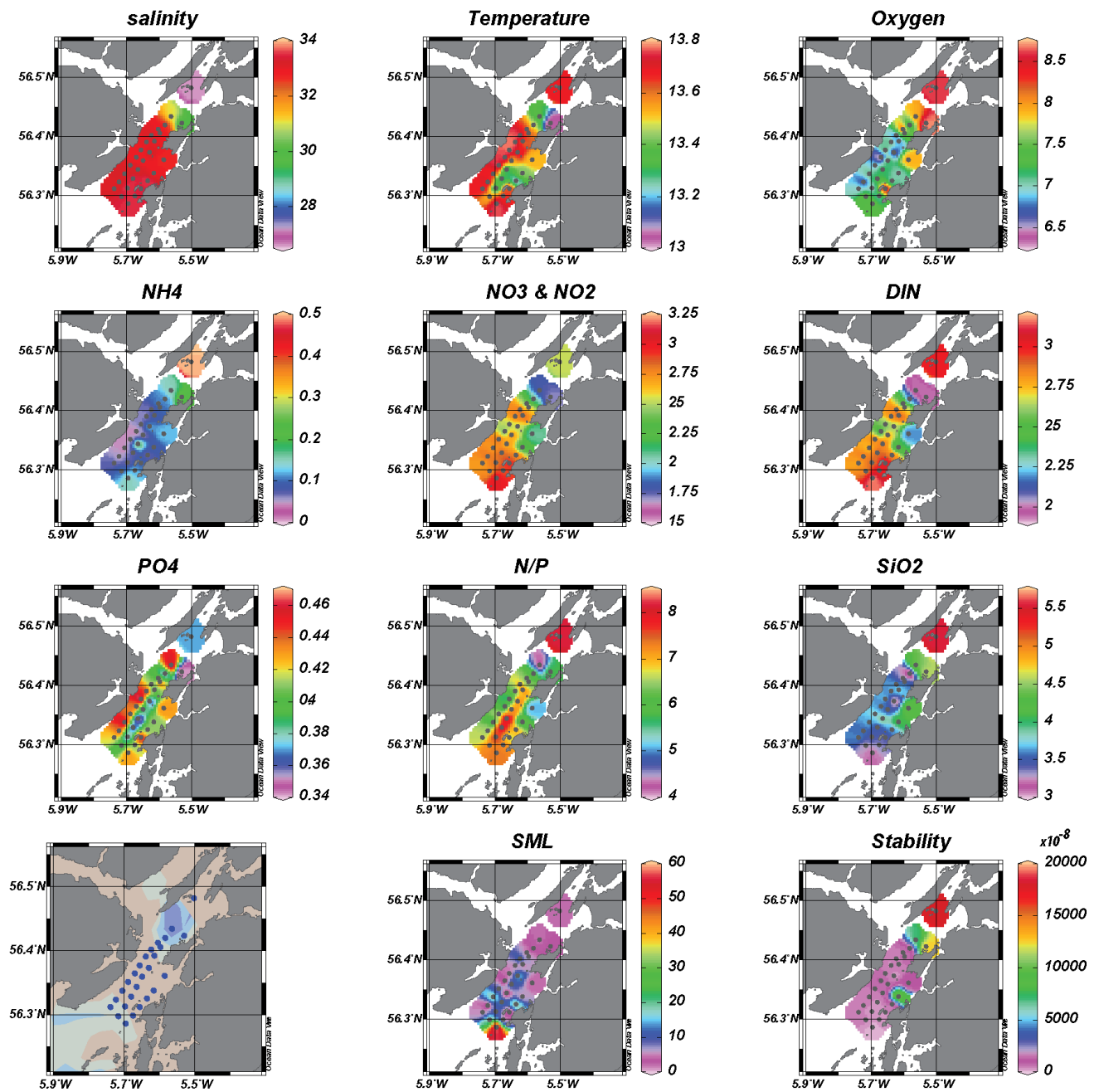


Figure 3 – Spatial distribution of surface salinity, temperature ($^{\circ}\text{C}$), oxygen ($\text{mg}\cdot\text{L}^{-1}$), NH_4 (μM), NO_3+NO_2 (μM), DIN (μM), PO_4 (μM), N/P ratio, SiO_2 (μM), Surface Mixed Layer depth (SML; m) and Stability ($\text{rad}^2\cdot\text{m}^{-1}$) in the Firth of Lorn. Note scales are different. Sampling stations are represented as blue dots in the bottom left plot.

Generally, temperatures at the surface were found to be lower in the east side of Firth of Lorn. The lowest temperatures ($\sim 13.0^{\circ}\text{C}$) were observed in front of the Oban bay (Figure 1) and from the island of Kerrera towards the open ocean (Figure 3). The lowest oxygen concentrations ($\sim 6.4\text{ mg}\cdot\text{L}^{-1}$) were found in the areas with higher temperatures, except in the most inner station, where temperatures ($\sim 14^{\circ}\text{C}$) and oxygen concentrations ($\sim 8.6\text{ mg}\cdot\text{L}^{-1}$) were the highest. The highest dissolved inorganic nitrogen concentrations were observed

in the most inner stations ($\sim 3.0 \mu\text{M}$) and in the most offshore stations ($\sim 3.6 \mu\text{M}$) of the Firth. Ammonium concentrations ($\sim 0.5 \mu\text{M}$) were observed to be the highest in the inner station and nitrate+nitrite was the main nitrogen compound ($\sim 3.1 \mu\text{M}$) in the offshore stations. Phosphate concentrations increased towards the open sea, especially in the west side of the Firth of Lorn ($\sim 0.45 \mu\text{M}$). The stations with the highest N/P ratio (~ 8) were the ones where nitrogen concentrations were largest, i.e. the most inner than the most offshore ones. The highest concentrations of silicate (SiO_2) were observed in the most inner station ($\sim 5.5 \mu\text{M}$) with concentrations decreasing towards the most offshore stations. The minimum silicate concentration observed in this study was $\sim 3.0 \mu\text{M}$. The depth of the SML was low in the most inner stations (2-5 m). The depth of SML varied between 2 and 19 m in the central area of the study region, with the highest values observed at the most offshore station (~ 60 m) at the southwest side, where the highest concentrations of nitrate and nitrite were also observed. The highest stability values were found in the most inner stations.

3.2 *Phytoplankton assemblages*

3.2.1 HPLC pigments and CHEMTAX

The highest concentrations of chlorophyll *a* ($\sim 2.6 \text{ mg}\cdot\text{m}^{-3}$) were found in the vicinity of Oban Bay and associated with a community dominated by flagellates such as dinoflagellates, haptophytes (hapto-6 and hapto-7), prasinophytes and cryptophytes (Figure 4). Pigment analysis indicated that the cryptophytes were the group that contributed the most to this peak of chlorophyll *a* ($\sim 1 \text{ mg}\cdot\text{m}^{-3}$) and generally the dominant group throughout the study area. The highest concentrations of chlorophyll *a* associated with diatoms were found in the most inner station of this study ($\sim 0.28 \text{ mg}\cdot\text{m}^{-3}$). The group hapto-8 yielded a peak in chlorophyll *a* in the middle of the Firth of Lorn. Generally, all these groups, except diatoms, were also found to be in high concentrations in the most inner stations and south of the island of Kerrera towards the open sea.

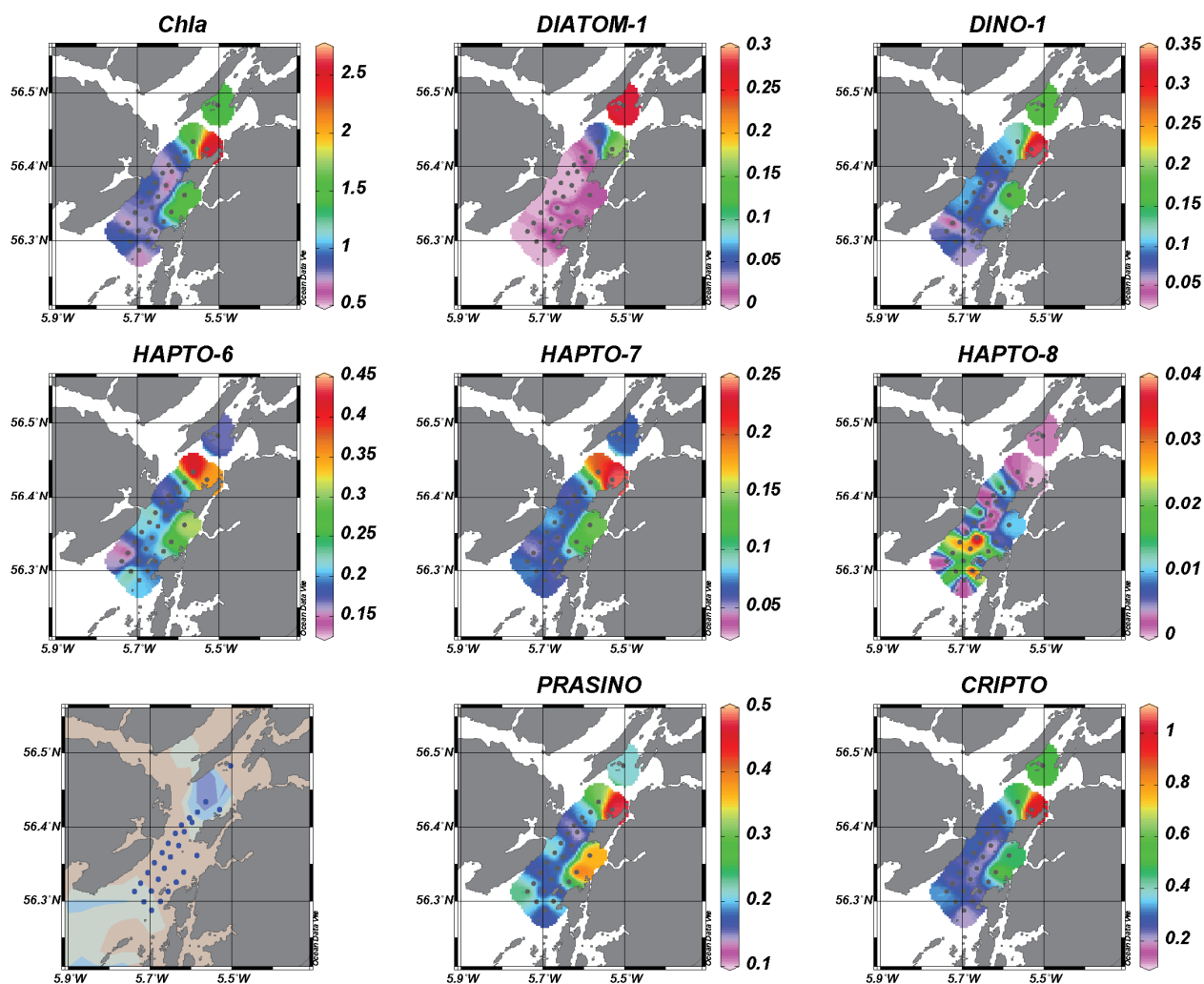


Figure 4 – Spatial distribution of chlorophyll *a* ($\text{mg}\cdot\text{m}^{-3}$) and the chlorophyll *a* concentrations associated with the following groups: diatoms-1, dinoflagellates-1, haptophytes-6, haptophytes-7, haptophytes-8, prasinophytes and cryptophytes. Contribution of phytoplankton groups to total chlorophyll *a* was obtained through CHEMTAX. Sampling stations are represented as blue dots in the bottom left plot.

3.2.2 Phytoplankton community: microscopy

Results obtained from microscopy were generally in agreement with pigment analysis. Cryptophytes were found to be the most abundant group throughout the study area (Figure 5). The highest abundances of dinoflagellates and cryptophytes were found near Oban Bay (59×10^3 and $\sim 190 \times 10^3 \text{ cells}\cdot\text{L}^{-1}$, respectively), as well as in the area south of the Sound of Kerrera to the open sea (37×10^3 and $\sim 54.5 \times 10^3 \text{ cells}\cdot\text{L}^{-1}$, respectively). The highest abundances of other flagellates (4.5×10^3 to $8 \times 10^3 \text{ cells}\cdot\text{L}^{-1}$) were observed in the most inner stations, however, nanoflagellates may be underestimated due to the difficulty in correctly identifying them by microscopy. Centric diatoms were found to have the highest

abundances at the most inner station ($\sim 110 \times 10^3$ cells.L⁻¹). The highest abundances of pennate diatoms were observed at the most inner ($\sim 3.3 \times 10^3$ cells.L⁻¹) and most offshore ($\sim 3.8 \times 10^3$ cells.L⁻¹) stations.

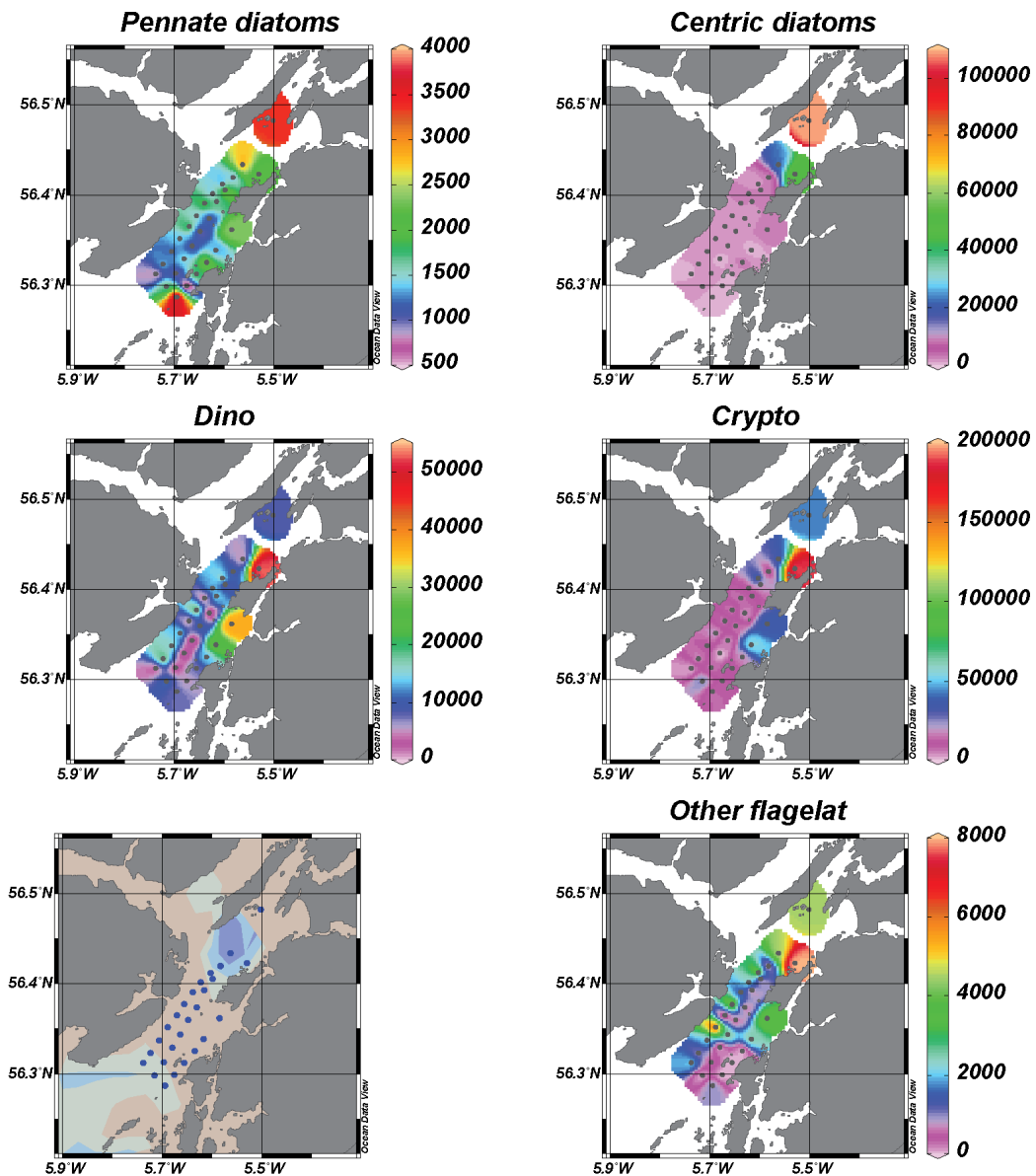


Figure 5 – Spatial distribution of phytoplankton cell abundances (cells.L⁻¹), obtained by microscopy, of the following groups: pennate diatom, centric diatoms, dinoflagellates and cryptophytes and other flagellates. Note the different scales. Sampling stations are represented as blue dots in the bottom left plot.

The highest abundances of *Chaetoceros* sp. and *Skeletonema costatum* (8.1×10^3 and 99.5×10^3 cells.L⁻¹, respectively) were recorded in the most inner station (Figure 6; Table 3). Their spatial distribution is in agreement with the general distribution of centric diatoms presented above. However, the distribution of *Paralia sulcata* is different, showing patches

throughout the Firth of Lorn and low abundances in the most inner stations. The pennate diatom *Cylindrotheca closterium* is well distributed across the Firth, with higher abundances in the most inner (2.4×10^3 cells.L⁻¹) and offshore (1.9×10^3 cells.L⁻¹) stations. *Nitzschia* sp. was mainly observed in the most southern station (1.0×10^3 cells.L⁻¹). Dinoflagellates were most abundant in front of Oban bay, where *Gymnodinium*-like cells reached abundances of $\sim 52 \times 10^3$ cells.L⁻¹.

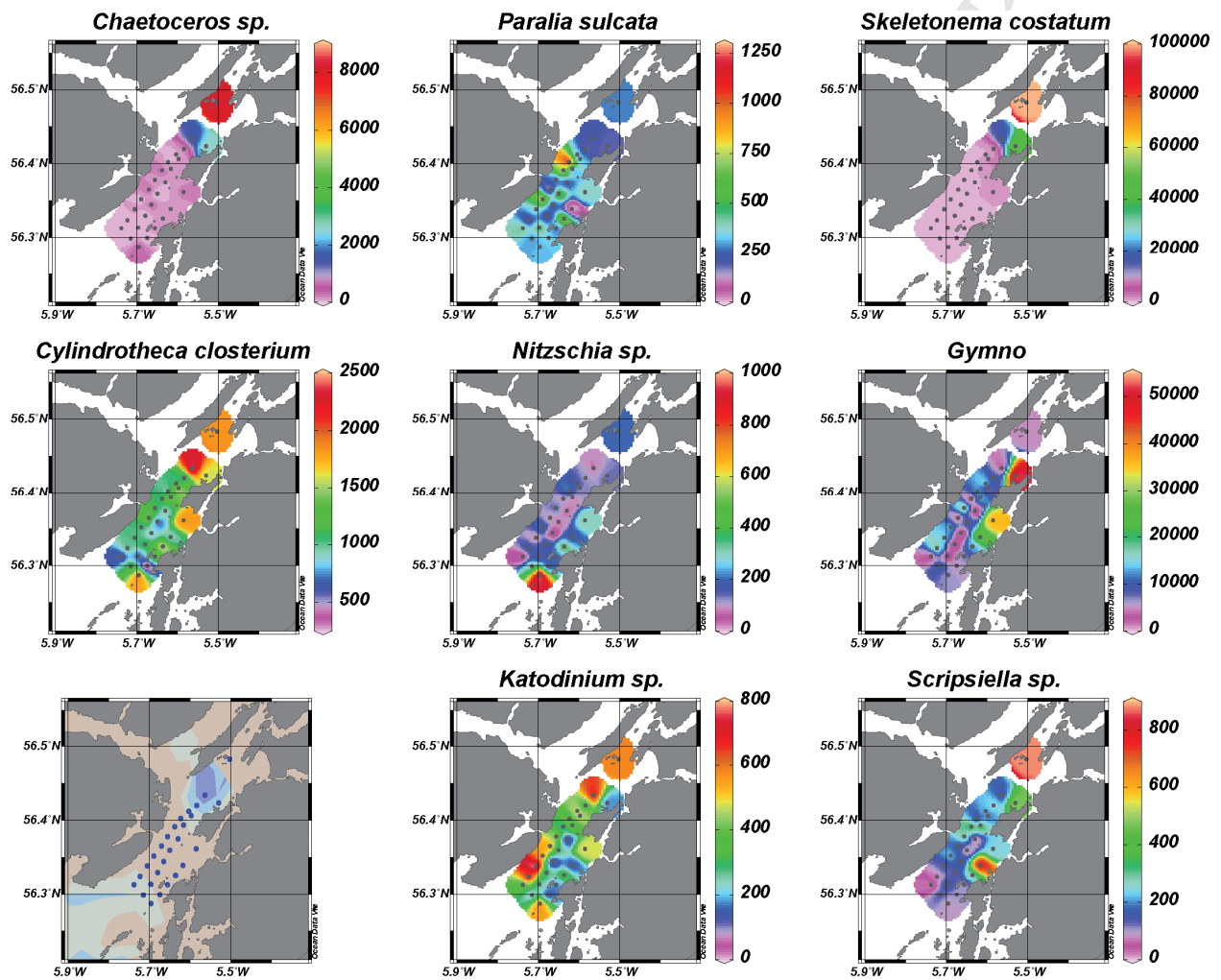


Figure 6 – Spatial distribution of phytoplankton cell abundances (cells.L⁻¹), obtained by microscopy, of the following taxa: 1) *Chaetoceros* sp., *Paralia sulcata* and *Skeletonema costatum* (centric diatoms); 2) *Cylindrotheca closterium* and *Nitzschia* sp. (pennate diatoms); and 3) *Gymnodinium*-like, *Katodinium* sp. and *Scripsiella* sp. (dinoflagellates). Note the different scales. Sampling stations are represented as blue dots in the bottom left plot.

3.3 HPLC-CHEMTAX vs cell counting

Good agreement was obtained from the direct comparison between phytoplankton cell counts and the contribution to total chlorophyll a obtained through HPLC-CHEMTAX ($p < 0.05$; Figure 7). All coefficients of determination were higher than 0.55 (e.g. $r^2 = 0.58$ for dinoflagellates). The highest coefficients were obtained for diatoms ($r^2 = 0.93$). Coefficients of determination of 0.87 and 0.74 were obtained for microphytoplankton (diatoms + dinoflagellates) and flagellates, respectively (Figure 7). Considering cryptophytes alone, which correspond to 85% of flagellate cell counts, a coefficient of determination of 0.85 was obtained (data not shown). For low abundances of diatoms, lower than 2×10^4 cells.L⁻¹, or chlorophyll a contributions lower than 0.04 mg.m^{-3} , a significant relationship between microscope and pigment data was not observed.

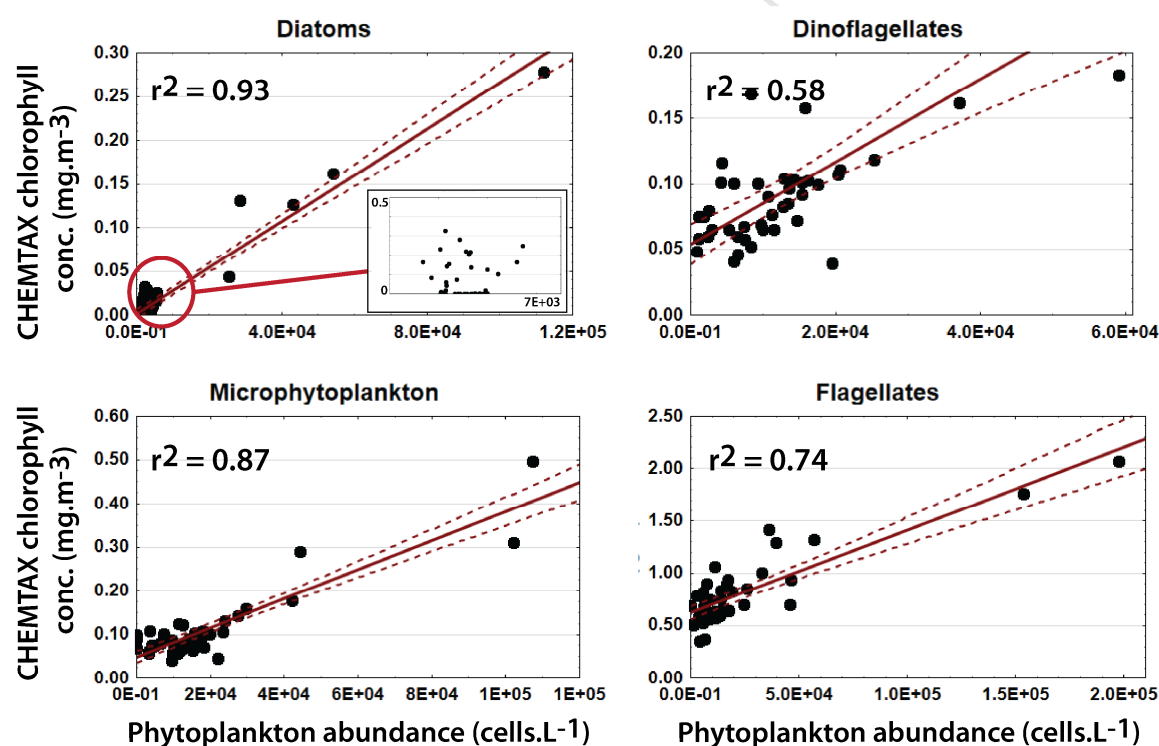


Figure 7 – Phytoplankton abundances (cells.L⁻¹) against chlorophyll a concentrations (mg.m^{-3}) obtained through CHEMTAX for diatoms, dinoflagellates, microphytoplankton (diatoms + dinoflagellates) and flagellates. Using CHEMTAX, flagellates were calculated by the sum of haptophytes, cryptophytes and prasinophytes. Microscopy counts included mostly cryptophytes and non-identified flagellates. The coefficients of determination are also presented.

3.4 Phytoplankton response to environmental drivers

A Canonical Correspondence Analysis (CCA) was used to investigate the response of the phytoplankton community (abundances data for all taxa) to the environmental variables observed in this study (Figure 8). A Monte Carlo test showed that six environmental variables explained significantly the variability of phytoplankton data (p -value < 0.025). Results are presented for microscopy data only, given that the CCA analysis for groups derived from CHEMTAX was not significant.

Using microscopy data, the CCA explained 90.3% of the variance associated with the phytoplankton-environment relationship. The first canonical axis alone explained 71.0% of the variance. The analysis indicated that centric diatoms responded to ammonium (NH_4) and silicate (SiO_2). They were also found to be negatively associated with salinity. Pennate diatoms and dinoflagellates were associated with high concentrations of nitrate+nitrite (NO_3+NO_2), phosphate (PO_4), temperature, as well as high salinities. Nevertheless, the influence of these environmental variables is stronger for pennate diatoms than for dinoflagellates. Cryptophytes were found to be negatively associated with nutrients in general, N/P ratio and temperature.

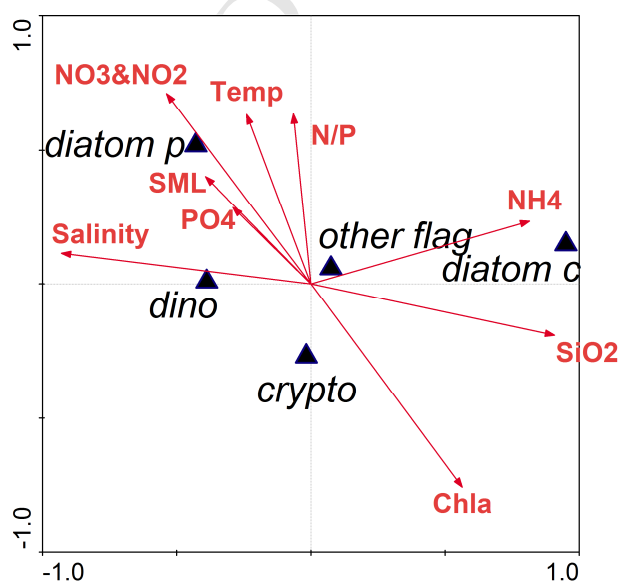


Figure 8 - Canonical Correspondence Analysis ordination diagram relative to data on absolute contributions of phytoplankton. The first two ordination axes represent 45.0% of the total phytoplankton variance and 90.3% of phytoplankton-environment relations. Arrows refer to environmental variables (Temperature, salinity, SML, NO_3+NO_2 , NH_4 , PO_4 , N/P and SiO_2). Variables used were: Diatom p- pennate diatoms; diatom c- centric diatoms; dino- dinoflagellates; crypto- cryptophytes; other flag- other flagellates.

A Canonical Correspondence Analysis (CCA) was also used to investigate the response of the eight most abundant phytoplankton taxa, within the diatom and dinoflagellate groups, to the environmental variables observed in this study (Figure 9). Each species contributed at least 0.75% of the total phytoplankton abundance observed in this study. A Monte Carlo test showed that six environmental variables contributed significantly to explain the variability of phytoplankton data (p -value < 0.03). The CCA explained 84.3% of the variance associated with the phytoplankton-environment relationship. The first canonical axis alone explained 71.6% of the variance. The centric diatoms *Chaetoceros* sp. and *Skeletonema costatum* were found to be associated with high concentrations of ammonium and silicate. The centric diatom of genus *Paralia* was observed to have an opposite relationship with these environmental variables, being strongly associated with high salinity, temperature, and high nitrate and phosphate concentrations, and negatively associated with ammonium and silicate. The pennate diatoms *Cylindrotheca closterium* and *Nitzschia* sp., as well as the dinoflagellates *Gymnodinium*-like and *Katodinium* sp. were also found to be influenced by high values of salinity and temperature, and high concentrations of nitrate and phosphate. High abundances of the dinoflagellate *Scrippsiella* sp. were found to be associated with low salinities and temperatures, as well as high phosphate and low nitrate concentrations

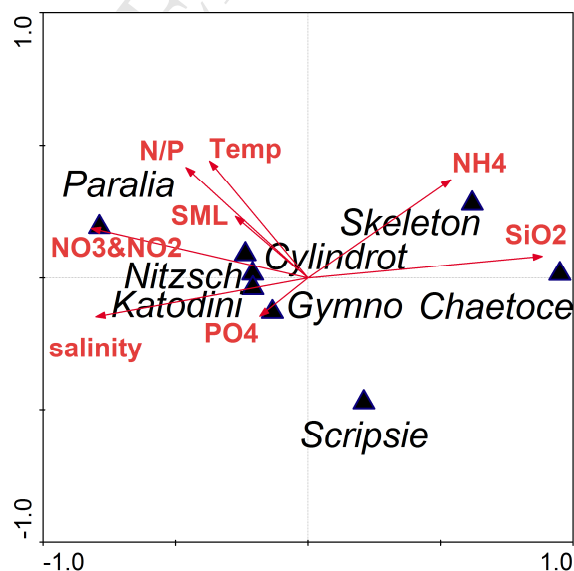


Figure 9 - Canonical Correspondence Analysis ordination diagram relative to data on absolute contributions of phytoplankton community, for the eight most abundant diatoms and dinoflagellates taxa. The first two ordination axes represent 34.2% of the total phytoplankton variance and 84.3% of phytoplankton-environment

relations. Arrows refer to environmental variables (Temperature, salinity, SML, NO_3+NO_2 , NH_4 , PO_4 , N/P and SiO_2). Variables used were: Chaetoce- *Chaetoceros*; Cylindrot- *Cylindrotheca*; Gymno- *Gymnodinium*-like; Katodini- *Katodinium*; Nitzsch- *Nitzschia*; Paralia- *Paralia*; Scripsie- *Scripsiella*; Skeleton- *Skeletonema*.

4. Discussion

4.1 HPLC-CHEMTAX vs Microscopy

Several studies have compared pigment chemotaxonomy (using CHEMTAX software) and microscopic analysis of phytoplankton groups and most of them suggested that it is crucial to combine both approaches to have a better understanding of the structure and functioning of phytoplankton communities (e.g., Schlüter et al., 2000; Havskum et al., 2004; Llewellyn et al., 2005; Kozłowski et al., 2011; de Souza et al., 2011; Mendes et al., 2011). The determination of photosynthetic pigment concentrations by HPLC, besides providing an accurate quantification of chlorophyll *a* concentration, allows the study of phytoplankton assemblage composition and structure, since some carotenoids and chlorophylls can be used as taxonomic indicators of phytoplankton groups (Gieskes and Kraay, 1983; Schlüter and Havskum, 1997; Ediger et al., 2006). However, interpretation of pigment data can be difficult as some pigments are present in several algal groups. For instance, fucoxanthin, which is a major pigment in diatoms, is also present in haptophytes (Jeffrey and Vesk, 1997; Wright and Jeffrey, 2006), and this can affect the estimation of diatoms by the CHEMTAX program. This problem of non-specificity of some pigments may have been the cause of the poor correlation observed for the stations with low contributions of diatoms. Another reason that may have contributed to this dissimilarity was microscopic enumeration of dead diatom cells that would not have been detectable in terms of pigments. Although this distinction was considered in the microscope counting, the separation between living and dead diatoms is very difficult (Schmid et al., 1998). It is recognized that microscope observations provide important taxonomical information (to species or genus), which provides a better taxonomic resolution than HPLC, particularly for large and recognizable organisms. Small-sized organisms, such as nanoplanktonic cells (e.g., haptophytes and prasinophytes) that were common in most of the stations of the studied region, are often difficult to preserve (not resistant to fixatives) and to identify by light microscopy. Therefore, microscopy can produce reliable identification of large cells, but often pico- and nanoplankton cells are unidentified or even overlooked. For this reason, using microscopy it

was not possible to obtain a good discrimination of most groups of pico- and nanoflagellates such as prasinophytes and/or haptophytes. However, despite all limitations considered, good agreements were found between microscope observations and pigment HPLC information for larger cells. Thus, the HPLC-CHEMTAX and microscopy were used in this study in a complimentary fashion, the first providing valuable information about the whole phytoplankton community, including small-size groups, whereas microscopy provided a good taxonomic reliability for large and recognizable organisms.

4.2 *Oban Bay: High biomass and low nutrients*

High chlorophyll *a* concentrations were found in the most inner stations, as well as in the area located between the islands of Kerrera and Seil. These areas correspond to the locations where the water column depth was the shallowest. The maximum depth of the water column was between 25 and 50m in those locations. From these, the highest chlorophyll *a* concentrations ($> 2 \text{ mg}\cdot\text{m}^{-3}$), were found in the station located next to Oban bay. Cryptophytes, which was the group that contributed the most to the high levels of biomass, is discussed in the next section. Physico-chemical conditions at this station were different from those observed elsewhere. At the surface ($\sim 5\text{m}$), the water temperature was found to be the lowest ($\sim 13.2^\circ\text{C}$) and oxygen concentration was the highest ($\sim 7.8 \text{ mg}\cdot\text{L}^{-1}$), of the whole sampling campaign. Salinity values were approximately 29.8 psu, lower than most values observed throughout the Firth of Lorn. These conditions suggest a significant influence of waters outflowing from the mouth of loch Eive, which is located near to this station. In this study, there are no data from this loch to confirm this influence. However, given that different conditions were found at the station located at the mouth of loch Linnhe, the other important source of freshwater for this region, loch Eive seems to be the most likely source for the fresher water mass observed in front of Oban Bay. Loch Eive exhibits a classical fjordic three-layer hydrodynamics with strong stratification (Gillibrand et al., 2013). It is therefore hypothesised that the water column at this location is not only influenced by waters from the surface layer ($< 10\text{m}$; McKee et al., 2002) of loch Eive, but it is, at least partly, influenced by waters from intermediate layers. Temperatures were much lower than what was observed in the surface waters near the mouth of loch Linnhe and salinities were higher than the ones found near the mouth of loch Linnhe. Previous studies (e.g. Edwards and Edelsten, 1977; Austin and Inall, 2002) have discussed that water renewal

events in loch Etive may contribute to a rapid change of temperature (1 to 2 °C) and salinity (1 unit of salinity). Nitrogen and phosphate concentrations in Oban Bay were observed to be amongst the lowest of the region. This may be the result of increased nutrient uptake by the high levels of phytoplankton biomass.

4.3 Phytoplankton response to environmental drivers

According to the CHEMTAX analysis, the highest abundance of diatoms (using the chlorophyll *a* concentration associated with diatoms as a proxy for abundance) was found in the most inner station. Microscopy allowed the discrimination of two diatom groups: pennate and centric, with their spatial distribution and response to environmental conditions being very different. Centric diatoms, such as *Chaetoceros* sp., *Skeletonema costatum* and *Paralia* sp. were found in the most inner stations of the Firth, especially at the mouth of Loch Linnhe. This group, which was the main component of diatoms' chlorophyll *a*, was found to be associated with high concentrations of ammonium and silicate, as well as low values of SML depth and salinity, as revealed by the CCA (Figure 8). Fehling et al. (2006) studied the temporal variation of the non-centric diatom *Pseudo-nitzschia*, from 2000 to 2003 at exactly the same location where these centric diatoms were observed, i.e. at the mouth of Loch Linnhe. It is interesting to note that diatom *Pseudo-nitzschia* cells were found to be associated with high concentrations of ammonium and low concentrations of nitrate and phosphate, as found for centric diatoms in this study. However, they were also found to be associated with high values of salinity and low concentrations of silicate (Fehling et al., 2006), which is different from what was observed in this station for centric diatoms, but similar to what was observed in other locations for pennate diatoms, which is discussed below.

At the species level, the CCA analysis confirmed that *Chaetoceros* sp. and *Skeletonema costatum* (centric diatoms) were favoured by high concentrations of ammonium and silicate, and were associated with low values of salinity and SML. Through a Redundancy analysis (RDA), Fehling et al. (2012) also reported similar relationships between *Chaetoceros* spp. and environmental parameters for the Scottish continental shelf. *S. costatum* species seem to prefer semi-enclosed environments (Smayda, 1957). This species has also been associated with stratified conditions in Scottish (Tett et al., 1986)

and Chilean (Alves-de-Souza et al., 2008) fjords. Conway and Harrison (1977) noted that the ability of *Skeletonema costatum* to take up ammonium is greater than that of *Chaetoceros* sp. However, the pattern is the opposite for silicate (Conway and Harrison, 1977), underpinning the stronger association between *Chaetoceros* sp. and silicate in this CCA analysis (Figure 9) and also observed by Fehling et al. (2012). Alves-de-Souza et al. (2008) also reported a strong association between *S. costatum* and silicate concentrations and Yoder (1979) indicated that silicate could be one of the most important limiting nutrients for *S. costatum*. This supports the confined distribution of these centric diatoms, which were mainly found where silicate concentrations were the highest.

Paralia sp. was the only centric diatom that did not follow the above pattern. It was associated with high nitrate, nitrite and phosphate concentrations, as well as high salinity values. It is interesting to note that Gerbühr et al. (2009), using data collected in the North Sea, from 1968 to 2005, presented similar results for *Paralia sulcata*. However, most studies also observe a strong association with silicate concentrations, most likely due to the heavily silicified nature of the valves of *Paralia* (e.g. McQuoid and Nordber, 2003). This relationship was not observed in the Firth of Lorn, where *Paralia* sp. was found to be strongly associated with low silicate concentrations. However, it is important to keep in mind that phytoplankton response may be delayed for some days, hence, significant phytoplankton growth may be observed when nutrient levels are already depleted (Davidson et al. 1992; Davidson et al. 1993) due to previous cell uptake. The clarification of this issue requires further investigation.

Pennate diatoms were found to be associated with high salinities, high concentrations of nitrate, nitrite and phosphate, as well as high SML depths (CCA). Using species data, the CCA analysis confirmed the response pattern for *Nitzschia* sp. and *Cylindrotheca closterium*. Fehling et al. (2012) observed a strong relationship between *Cylindrotheca closterium* and *Pseudo-nitzschia delicatissima* and high salinity waters with high nitrogen concentrations. Salinity acting as a marker of oceanic water masses that work as a source of nitrogen (Fehling et al., 2012). Alves-de-Souza et al. (2008) also reported the association between a group of pennate diatoms (e.g. *Cylindrotheca closterium*, *Pseudo-nitzschia* spp. and *Leptocylindrus minimus*) and high concentrations of nitrate and phosphate. *Cylindrotheca closterium* responds quickly to nutrient enrichment and is frequently found in turbulent and mixed waters, during upwelling events (e.g. Moita et al., 2003; Brito et al.,

2012a; Hansen et al., 2014). The most offshore station, where the peak of pennate diatoms was found, had a deep SML depth (~ 60m), which is likely to be a consequence of the mixed influence of the Great Race (Dale et al., 2011) and the 1-week event of strong winds. The wind-driven mixing is likely to have caused the break down of the typical summer stratification (Lønborg et al., 2009; Fehling et al., 2012) at the most offshore locations, making nutrients available for phytoplankton growth. Concerning nutrients, these high salinity oceanic waters were found to have different chemical compositions. Such changes in the relative nutrient availability are likely to trigger modifications in the phytoplankton community. The strong flows through the Sound of Luing and the Gulf of Corryvreckan may also be responsible for the resuspension of microalgae cells from the seabed, which would thrive in a nitrate-enriched environment. Importance of microalgae resuspension has already been reported for shallower coastal areas (e.g. De Jonge and van Beusekom, 1995; Brito et al., 2012b). *Cylindrotheca closterium* is characterized as a thycoplanktonic species (i.e, present in benthic and pelagic environment) and within genera *Nitzschia* many species are considered benthic (e.g. Staats et al., 1999; Yamamoto et al., 2012).

The highest abundances of flagellates (dinoflagellates, haptophytes, prasinophytes and cryptophytes) were observed in front of Oban Bay. This station was stratified and was considered the most 'oligotrophic' area of the study region, given that it was the location where the lowest concentrations of both nitrogen and phosphate were recorded. Dinoflagellates were usually considered to be indicators of stratified waters, which seems to be the case of the station in front of Oban Bay. However, as noted above, Smayda and Reynolds (2001) suggested that dinoflagellates include species that use three different strategies, the C-, S- and R-strategies, to exploit existent environment conditions according to the onshore-offshore gradient. From these, gymnodinioid (i.e. *Gymnodinium*-like) species were the most abundant dinoflagellates in Oban Bay. Although the results of CCA do not show a strong association between Gymnodinioids and nutrients, they are considered a typical C-strategist (opportunistic colonist) from Type I habitat, which includes nutrient enriched shallow coastal waters with seasonal intense stratification (Smayda and Reynolds, 2001; 2003). This does not seem to be in agreement with what was observed in Oban Bay, except if deeper waters of loch Etive, which are likely to be nutrient enriched, were influencing Oban Bay station. In this case, it could be hypothesised that, at

the time of sampling, the observed high phytoplankton biomass was responsible for the removal of nutrients from these surface waters, which is not the most likely scenario given the occasional nature of these processes. It is also interesting to note that dinoflagellates were the group with less affinity to ammonium concentrations, which is in agreement with previous studies (e.g. Bhovichitra and Swift, 1977; Litchman et al., 2007). Moreover, one has to keep in mind that dinoflagellates are characterised by complicated trophic relationships, having mixotrophic feeding strategies (e.g. Spector, 1984; Nakamura et al., 1995).

The HAPTO-6 group (e.g. *Emiliana huxleyi*) was the most abundant group of haptophytes in this region. *Emiliana huxleyi* is considered to be a fast growing phytoplanktonic species, especially under eutrophic conditions (r-strategy; Tyrrell and Merico, 2004). The set of conditions that are ideal for a bloom of *Emiliana huxleyi* are not fully understood yet (Lessard et al., 2005). It has been reported that high N/P ratios, i.e. phosphate limitation, was one of the required conditions (Tyrrell and Merico, 2004; Lessard et al., 2005). However, more recent studies have reported that most blooms were observed under low N/P ratios (details in Lessard et al., 2005). In fact, the distribution of HAPTO-6 in our study seems to be related to the lowest N/P ratios found for the Firth of Lorn. However, as discussed by Davidson et al. (2012), the relationship between N/P ratio and phytoplankton functional groups can be difficult to interpret unless it can be clearly established that nutrient limitation is occurring.

HPLC-CHEMTAX is an essential methodology to identify small flagellates, which could otherwise, i.e. through microscopy, be neglected. This is the case for Prasinophytes, which is a group known to be common in temperate and cold waters (Not et al., 2004; Becker and Kirchgasser, 2007). Although being one of the most abundant groups of flagellates in the Firth of Lorn, in this study their small size meant they were not identified by microscopy. Given that reliable identification of Prasinophytes is generally difficult, little is known about the abundance and ecology of the members of this group (Gescher et al., 2008). Tappan (1980) named them as the 'disaster species' due to the reports of prasinophytes blooms during the decline of the 'normal' phytoplankton community. Hence, they have been considered an indicator of stressful environments. Here, the highest abundance of prasinophytes was observed in Oban Bay, which was the most nutrient depleted station at the time of sampling.

Cryptophytes, which were found in high abundances in the inner area of the Firth of Lorn, especially in Oban Bay, were the main group contributing to the total phytoplankton biomass observed in this region. They dominated the phytoplankton community at relatively stable and stratified locations, with low SML depth, low temperatures, low concentrations of nitrate, nitrite and phosphate (which increased towards open ocean), as well as high silicate concentrations (CCA analysis). The association of cryptophytes with high silicate concentrations may be an indicator that they respond to the input of freshwater leading to some degree of stratification. For instance, Moline et al. (2004) has shown the association between low salinity/stratified waters and cryptophytes, this was also observed by Mendes et al. (2013) in the Antarctic Peninsula, where the phytoplankton community was dominated by cryptophytes in areas receiving freshwater due to ice melting. Brito et al. (2014) also provided an indication of this relationship in temperate estuarine systems. Our results have shown that centric diatoms are favoured by high concentrations of ammonium and silicate and low salinity values, while cryptophytes seem to have a weak response to salinity and do not seem to be favoured by high concentrations of ammonium, as the ones observed in the most inner station of the Firth of Lorn. In general terms, no clear response of cryptophytes to nutrient enrichment was observed, as discussed by Balode et al. (1998), Arhonditsis et al. (2008) and Mendes et al. (2013). As for dinoflagellates, cryptophytes can also be mixotrophic, combining autotrophic with heterotrophic feeding strategies, especially during periods of low nutrient concentrations (Lee, 2008).

4.4 *Phytoplankton Functional Groups: an overview for diatoms*

Functional groups can be discriminated based on the relationship between maximum linear dimension and surface/volume ratio (S/V ; Reynolds, 1996). C- strategists would be the colonist, fast-growing species with small and high S/V cells, that dominate in stratified waters, as already discussed in the previous section. Species with R-strategy would be the elongated, high S/V species that thrive under turbulent conditions with high nutrient concentrations. S- strategists would be the slow-growing species with large cells that are adapted to oligotrophic conditions. Although diatoms are generally considered R-strategists,

Bonilla et al. (2005) discussed that some species, such as *Chaetoceros* spp., may be considered CR-strategists. In this study, *Chaetoceros* sp. was abundant in areas with low turbulence. Plots that compare DIN and S/V with SML depth yield results for *Chaetoceros* sp. that are similar with those of Gymnodinioid group, that is a typical C-strategist (Smayda and Reynolds, 2003; Figure 10). This is also in accordance to the flexible classification presented by Bonilla et al. (2005).

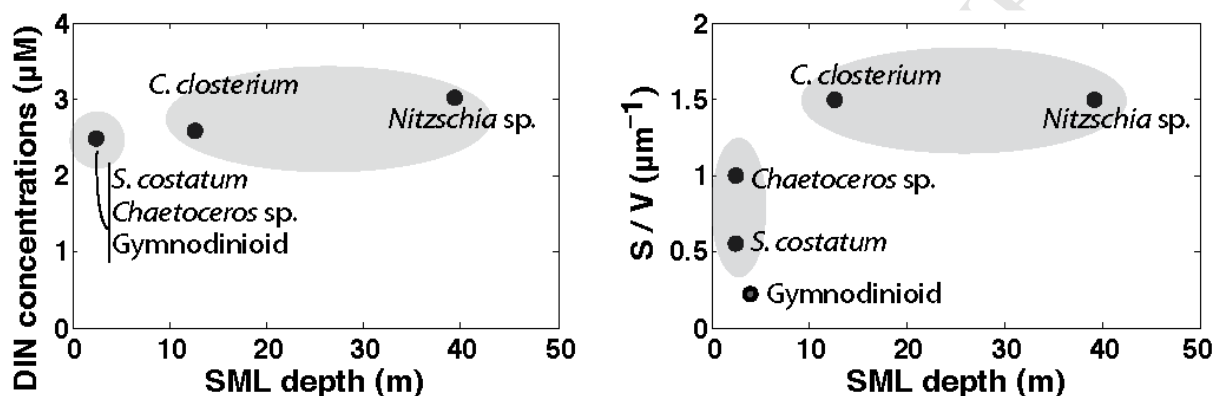


Figure 10 – A – DIN concentrations (μM) against SML depth (m) and B – S/V ratio (μm^{-1}) against SML depth (m) for two pennate species (*C. closterium* and *Nitzschia* sp.), two centric species (*S. costatum* and *Chaetoceros* sp.) and Gymnodinioids. Pennate and centric species are grouped in grey circles. DIN and SML data were collected during this study and S/V data for *S. costatum*, *C. closterium* and *Gymnodinium* sp. (for Gymnodinioids) were taken from Alves-de-Souza et al. (2008). S/V ratio of *Nitzschia* sp. was considered to be similar to *C. closterium*. S/V ratio of *Chaetoceros* sp. was considered to be an approximation to the average ratios of genus *Chaetoceros* presented by Alves-de-Souza et al. (2008).

Alves-de-Souza et al. (2008) presented one of the first studies applying Reynolds' model to marine diatom communities. They identified three functional groups of diatoms in the Chilean fjords: D1 composed of species with $S/V > 1.5 \mu\text{m}^{-1}$ and high correlation with nitrate (e.g. *C. closterium*); D2 composed of species with $S/V \sim 1 \mu\text{m}^{-1}$ and also correlated with nitrate (e.g. *Chaetoceros* sp.); and D3 composed of species with $S/V \sim 0.5-0.8 \mu\text{m}^{-1}$ and correlated with silicate and stratification (*S. costatum*). In addition to Alves-de-Souza et al. (2008), other studies such as Smayda and Boleyn (1966) in the Narragansett Bay (USA), Varela et al. (2011) in Saanich Intet (British Columbia, Canada) and Joint et al. (1987) in Loch Ewe (Western Scotland) have also reported S/V values of $\sim 0.6-0.9 \mu\text{m}^{-1}$ for *S. costatum*. With some differences, the results presented herein show great similarities with the ones reported by Alves-de-Souza et al. (2008; Figure 10). Although data used is temporally

restricted, providing only a quick snapshot of the seasonal pattern, in this study the existence of four groups of diatoms is hypothesized. Each group is represented by one species. Pennate and centric diatoms seems to be located in very distinctive areas of the plots presented in Figure 10, as well as responding to different environmental conditions, as discussed before. *Cylindrotheca closterium* and *Nitzschia* sp. yielded similar responses to environmental variables in the CCA. However, they were associated with very different mixing regimes, which may indicate inherent functional differences. *Chaetoceros* sp. and *S. costatum* were found in the same stratified conditions (similar SML depth). Their response to environmental variables is slightly different and their S/V ratio is also generally different. The S/V ratio is an important factor to differentiate functional groups as discussed by Reynolds et al. (2002) and Alves-de-Souza et al. (2008), as the separation of species by morphology coincides with their distribution throughout different habitats (Reynolds et al., 1997). Further studies considering the long-term dynamics of phytoplankton in the Firth of Lorn would be essential to test the hypothesis proposed here. In summary, one could hypothesize that pennate diatoms are composed of two functional groups, i.e. P1 (*C. closterium*) and P2 (*Nitzschia* sp.), and centric diatoms are composed of two groups as well, i.e. C1 (*S. costatum*) and C2 (*Chaetoceros* sp.).

5. Conclusions

Microscopy analysis of phytoplankton communities is able to provide good taxonomic resolution (species level) for large cells (> 20 μ m), however, pico and nanophytoplankton are often unidentified. Phytoplankton pigments, through the chemotaxonomical analysis, are considered decisive to identify the presence of groups of smaller cells. HPLC-CHEMTAX and microscopy should therefore be used complementarily to obtain information about the whole community.

Cryptophytes were the most abundant phytoplankton group in the Firth of Lorn, mainly at stratified stations, where SML depth, temperatures, and concentrations of nitrogen and phosphorus were low and concentrations of silicate were high. The most abundant dinoflagellates observed in this region were the *Gymnodinium*-like cells, which were also present in the stratified waters with low concentrations of nitrogen and phosphorus.

Centric diatoms, mainly *S. costatum* and *Chaetoceros* sp. were observed in the most inner stations of the region, which were stratified (with low SML depth) and had high concentrations of ammonium and silicate but low concentrations of nitrate and phosphate. The S/V ratio of centric diatoms was lower than those of pennate diatoms (*Cylindrotheca closterium* and *Nitzschia* sp.). Pennate diatoms were observed at stations with high concentrations of nitrate and phosphate and higher SML depths. SML depth was much higher for *Nitzschia* sp., which was found in more turbulent conditions than for *C. closterium*. Four diatom groups were therefore proposed according to their surface to volume ratios, turbulence and preferred nutrient conditions.

6. Acknowledgments

The authors are deeply indebted to all people who assisted during sampling and laboratory work at SAMS. Special thanks to Sharon McNeill (SAMS). We are grateful to Simon Wright, from the Australian Antarctic Division, for providing CHEMTAX v.1.95.

Ana C. Brito was funded by a Portuguese Post-doc grant from Fundação para a Ciência e a Tecnologia (FCT; BPD/63017/2009) and FCT Investigador Programme (IF/00331/2013). Carolina Sá received a PhD grant from FCT (BD/24245/2005) and an additional grant from the EU FP7 AQUA-USERS (FP7-607325). Carlos R. Mendes was funded by a postdoc grant from CAPES (Brazil). Keith Davidson was in receipt of funding from the NERC Shelf Seas Biogeochemistry programme.

This study was conducted in the framework of EU ASSEMBLE Project (FP7-227799) and also received support by FCT (PEst-OE/MAR/UI0199/2014).

7. References

- Adams, T.P., Miller, R.G., Aleynik, D., Burrows, M.T. (2014). Offshore marine renewable energy devices as stepping stones across biogeographical boundaries. *Journal of Applied Ecology*, in press.
- Alves-de-Souza, C., Gonzalez, M.T., Uriarte, J.L. (2008). Functional groups in marine phytoplankton assemblages dominated by diatoms in fjords of Southern Chile. *Journal of Plankton Research*, 11, 1233-1243.
- Arhonditsis, G.B., Stow, C.A., Paerl, H.W., Valdes-Weaver, L.M., Steinberg, L.J., Reckhow, K.H. (2007). Delineation of the role of nutrient dynamics and hydrologic forcing on phytoplankton patterns along freshwater-marine continuum. *Ecological Modelling*, 208, 230-246.
- Austin, W.E.N., Inall, M. (2002). Deep-water renewal in a Scottish fjord: temperature, salinity and oxygen isotopes. *Polar Research*, 21, 251-258.

- Balode, M., Purina, I., Béchemin, C.H., Maestrini, S. (1998). Effects of nutrient enrichment on the growth rates and community structure of summer phytoplankton from the gulf of Riga, Baltic Sea. *Journal of Plankton Research*, 20, 2251-2272.
- Bhovichitra, M., Swift, E. (1977). Light and dark uptake of nitrate and ammonium by large oceanic dinoflagellates: *Pyrocystis noctiluca*, *Pyrocystis fusiformis* and *Dissodinium lunula*. *Limnology and Oceanography*, 22, 73-83.
- Bonilla, S., Conde, D., Aubriot, L., Pérez, M.C. (2005). Influence of Hydrology on Phytoplankton Species Composition and Life Strategies in a Subtropical Coastal Lagoon Periodically Connected with the Atlantic Ocean. *Estuaries*, 28, 884-895.
- Brainerd, K. E., and M. C. Gregg (1995). Surface mixed and mixing layer depths. *Deep-Sea Research*, 42A, 1521-1543.
- Brito, A.C., Quental, T., Coutinho, T.P., Branco, M.A.C., Falcão, M., Newton, A., Icely, J., Moita, T. (2012a). Phytoplankton dynamics in southern Portuguese coastal lagoons during a discontinuous period of 40 years: an overview. *Estuarine, Coastal and Shelf Science*, 110, 147-156.
- Brito, A.C., Fernandes, T.F., Newton, A., Facca, C., Tett, P. (2012b). Does microphytobenthos resuspension influence phytoplankton in shallow systems? A comparison through a Fourier series analysis. *Estuarine, Coastal and Shelf Science*, 110, 72-84.
- Brito, A.C., Moita, T., Gameiro, C., Silva, T., Anselmo, T., Brotas, V. (2014). Changes in the Phytoplankton Composition in a Temperate Estuarine System (1960 to 2010). *Estuaries and Coasts*, in press.
- Chrétiennot-dinet, M. (1990). *Atlas du Phytoplancton Marin. III. Chlorarachniophycées, Chlorophycées, Chrysophycées, Cryptophycées, Euglénophycées, Eustigmatophycées, Prasinophycées, Prymnesiophycées, Rhodophycées et tribophycées*. Centre National de la Recherche Scientifique. Paris. France.
- Conway, H.L., Harrison, P.J. (1977). Marine diatoms grown in chemostats under silicate or ammonium limitation. IV. Transient response of *Chaetoceros debilis*, *Skeletonema costatum* and *Thalassiosira gravida* to a single addition of the limiting nutrient. *Marine Biology*, 43, 33-43.
- Dale, A.C., Boulcott, P., Shewin, T.J. (2011). Sedimentation patterns caused by scallop dredging in a physically dynamic environment. *Marine Pollution Bulletin*, 62, 2433-2441.
- de Souza, M.S., Mendes, C.R.B., Garcia, V.M.T., Pollery, R., Brotas, V. (2011). Phytoplankton community during a coccolithophorid bloom in the Patagonian shelf: microscopic and high-performance liquid chromatography pigment analyses. *Journal of the Marine Biological Association of the United Kingdom*, 92, 13-27.
- Davidson, K., Flynn, K.J., Cunningham, A. (1992). Non-steady state ammonium-limited growth of the marine phytoflagellate *Isochrysis galbana* Parke. *Ney Phytologist*, 122, 433-438.
- Davidson, K., Cunningham, A., Flynn, K.J. (1993). Modelling temporal decoupling between biomass and numbers during the transient nitrogen-limited growth of a marine phytoflagellate. *Journal of Plankton Research*, 15, 351-359.

- Davidson, K., Gowen, R.J., Tett, P., Bresnan, E., Harrison, P.J., McKinney, A., Milligan, S., Mills, D.K., Silke, J., Crooks, A-M. (2012). Harmful algal blooms: How strong is the evidence that nutrient ratios and forms influence their occurrence? *Estuarine, Coastal and Shelf Science*, 115, 399-413.
- Davidson, K., Gowen, R.J., Harrison, P.J., Fleming, L.E., Hoagland, P., Moschonas, G. (2014). Anthropogenic nutrients and harmful algae in coastal waters. *Journal of Environmental Management*, 146, 206-216.
- De Jonge, V., van Beusekom, J.E. (1995). Wind- and tide-induced resuspension of sediment and microphytobenthos from tidal flats in the Ems estuary. *Limnology and Oceanography*, 40, 776-778.
- Diamond, D. (2003). Determination of silicate in brackish or seawater by flow injection analysis. *QuikChem Method*, 31-114-27-1-A
- Diamond, D. (2008). Determination of nitrate/nitrite in brackish or seawater by flow injection analysis *QuikChem Method* 31-107-04-1-A
- Ediger, D., Soydemir, N., Kideys, A.E. (2006). Estimation of phytoplankton biomass using HPLC pigment analysis in the southwestern Black Sea. *Deep-Sea Research II*, 53, 1911-1922.
- Edwards, A. and Grantham, B. E. (1986). Inorganic nutrient regeneration in Loch Etive bottom water. In: *The Role of Freshwater Outflow in Coastal Marine Ecosystem*, NATO ASI Series G: Ecological Sciences, Vol. 7, Springer-Verlag, 195–204.
- Edwards, A., Baxter, M.S., Ellett, D.J., Martin, J.H.A., Meldrum, D.T. and Griffiths, C.R. (1986). Clyde Sea hydrography, *Proceedings of the Royal Society of Edinburgh*, 90B, 67–83.
- Egan, L. (2008). Determination of orthophosphate by flow injection analysis. *QuikChem Method*, 31-115-01-1-I
- Fehling, J., Davidson, K., Bolch, C., Tett, P. (2006). Seasonality of *Pseudo-nitzschia* spp. (Bacillariophyceae) in western Scottish waters. *Marine Ecology Progress Series*, 323, 91-105.
- Fehling, J., Davidson, K., Bolch, C.J.S., Brand, T.D., Narayanaswamy, B.E. (2012). The relationship between phytoplankton distribution and water column characteristics in North West European Shelf Sea Waters. *Plos One*, 7, 1-16.
- Gade, H.G. and Edwards, A. (1980). Deep-water renewals in fjords. In: H.J. Freeland, D.M. Farmer and C.D. Levings (eds.), *Fjord Oceanography*, Plenum pp. 453–489.
- Gaard, E., Nordi, G.A., Simonsen, K. (2011). Environmental effects on phytoplankton production in a Northeast Atlantic fjord, Faroe Islands. *Journal of Plankton Research*, 33, 947-959.
- Gebühr, C., Wiltshire, K.H., Aberle, N., van Beusekom, J.E.E., Gerds, G. (2009). Influence of nutrients, temperature, light and salinity on the occurrence of *Paralia sulcata* at Helgoland Roads, North Sea. *Aquatic Biology*, 7, 185-197.
- Gescher, C., Metfies, K., Frickenhaus, S., Kniefkamp, B., Wiltshire, K.H., Medlin, L.K. (2008). Feasibility of Assessing the Community Composition of Prasinophytes at the Helgoland Roads Sampling site with a DNA Microarray. *Applied and Environmental Microbiology*, 74, 5305-5316.
- Geyer, W.R., Cannon, G.A. (1982). Sill processes related to deep-water renewal in a fjord. *Geophysical Research*, 87, 7985-7996.

- Gieskes, W.W.C., Kraay, G.W. (1983). Dominance of Cryptophyceae during the phytoplankton spring bloom in the central North Sea detected by HPLC analysis of pigments. *Marine Biology*, 75, 179-185.
- Gillibrand, P.A., Inall, M.E., Portilla, E., Tett, P. (2013). A box model of the seasonal Exchange and mixing in Regions of Restricted Exchange: Application to two contrasting Scottish inlets. *Environmental Modelling and Software*, 43, 144-159.
- Grasshoff, K. *Methods of Seawater analysis*, Verlag Chemie, Second Edition, 1976
- Hansen, A., Ohde, T., Wasmund, N. (2014). Succession of micro- and nanoplankton groups in ageing upwelled waters off Namibia. *Journal of Marine Systems*, in press.
- Havskum, H., Schluter, L., Scharek, R., Berdalet, E., Jacquet, S. (2004). Routine quantification of phytoplankton groups - microscopy or pigment analyses? *Marine Ecology Progress Series*, 273, 31-42.
- Higgins, H.W., Wright, S.W., Schlüter, L. (2011). Quantitative interpretation of chemotaxonomic pigment data. In: Roy, S., Llewellyn, C.A., Egeland, E.S., Johnson, G. (Eds.), *Phytoplankton Pigments: Characterization, Chemotaxonomy and Applications in Oceanography*. Cambridge Uni. Press, pp. 257-313.
- Hoppenrath, M., Elbrächter, M. & Drebes, G.. 2009. *Marine Phytoplankton. Selected microphytoplankton species from the North Sea around Helgoland and Sylt*. E. Schweizerbart'sche Verlagsbuchhandlung. Stuttgart. Germany.
- IOC, SCOR, IAPSO (2010). The international thermodynamic equation of seawater – 2010: calculation and use of thermodynamic properties. Intergovernmental Oceanographic Commission, Manuals and Guides No. 56, UNESCO, 196pp.
- Jeffrey, S.W., Veski, M. (1997). Introduction to marine phytoplankton and their pigment signatures. In: Jeffrey SW, Mantoura RFC, Wright SW (Eds.), *Phytoplankton Pigments in Oceanography: guidelines to modern methods*, UNESCO Monogr. Oceanogr. Methodol., Vol 10, UNESCO Publishing, Paris, pp. 37-84.
- Joint, I.R., Pomroy, A.J., Robinson, G.A., Morris, R.J., McCartney, M.J. (1987). Morphological changes in *Skeletonema costatum* (Bacillariophyceae) during a spring bloom in a marine ecosystem enclosure. *British Phycological Journal*, 22, 119-124.
- Jones, K.J., Gowen, R.J. (1990). Influence of stratification and irradiance regime on summer phytoplankton composition in coastal and shelf seas of the British Isles. *Estuarine, Coastal and Shelf Science*, 30, 557-567.
- Kozłowski, W.A., Deutschman, D., Garibotti, I., Trees, C., Vernet, M. (2011). An evaluation of the application of CHEMTAX to Antarctic coastal pigment data. *Deep-Sea Research I*, 58, 350-364.
- Lee, R.E. (2008). *Phycology*. Cambridge University Press, 560pp.
- Lessard, E.J., Merico, A., Tyrrell, T. (2005). Nitrate:phosphate ratios and *Emiliania huxleyi* blooms. *Limnology and Oceanography*, 50, 1020-1024.
- Liao, N. (2008). Determination of ammonia in brackish or seawater by flow injection analysis. *QuikChem Method*, 31-107-06-1-B

- Litchman, E., Klausmeier, C. A., Schofield, O. M., Falkowski, P. G. (2007). The role of functional traits and trade-offs in structuring phytoplankton communities: scaling from cellular to ecosystem level. *Ecology Letters*, 10(12), 1170-1181.
- Llewellyn, C.A., Fishwick, J.R., Blackford, J.C. (2005). Phytoplankton community assemblage in the English Channel: a comparison using chlorophyll a derived from HPLC-CHEMTAX and carbon derived from microscopy cell counts. *Journal of Plankton Research*, 27, 103-119.
- Lønborg, C., Davidson, K., Álvarez-Salgado, X., Miller, A. (2009). Bioavailability and bacterial degradation rates of dissolved organic matter in a temperate coastal area during an annual cycle. *Marine Chemistry*, 113, 219-226.
- Lund, J.W.G., Kipling, C., Le Cren, E.D. (1958). The invert microscope method of estimating algal numbers and the statistical basis of estimations by counting. *Hydrobiologia*, 11 (2), 143-170.
- Mckee, D., Cunningham, A., Jones, K.J. (2002). Optical and hydrological consequences of freshwater run-off during Spring phytoplankton growth in a Scottish fjord. *Journal of Plankton Research*, 24, 1163-1171.
- Margalef, R. (1978). Life-forms of phytoplankton as survival alternatives in an unstable environment. *Oceanologica Acta*, 1, 493-509.
- Mackey, M., Mackey, D., Higgins, H., Wright, S. (1996). CHEMTAX - a program for estimating class abundances from chemical markers: application to HPLC measurements of phytoplankton. *Marine Ecology Progress Series*, 144, 265-283.
- Mendes, C.R., Cartaxana, P., Brotas, V. (2007). Determination of phytoplankton and microphytobenthos pigments: comparing resolution and sensitivity of a C18 and a C8 method. *Limnology and Oceanography: methods*, 5, 363-370.
- Mendes, C.R., Sá, C., Vitorino, J., Borges, C., Garcia, V.M.T., Brotas, V. (2011). Spatial distribution of phytoplankton assemblages in the Nazaré submarine canyon region (Portugal): HPLC-CHEMTAX approach. *Journal of Marine Systems*, 87, 90-101.
- Mendes, C.R., Tavano, V.M., Leal, M.C., de Souza, M.S., Brotas, V., Garcia, C.A.E. (2013). Shifts in the dominance between diatoms and cryptophytes during three late summers in the Bransfield Strait (Antarctic Peninsula). *Polar Biology*, 36, 537-547.
- McQuoid, M.R., Norberg, K. (2003). The diatom *Paralia sulcata* as an environmental indicator species in coastal sediments. *Estuarine, Coastal and Shelf Science*, 56, 339-354.
- Moita, T., Oliveira, P.B., Mendes, J.C., Palma, A.S. (2003). Distribution of chlorophyll a and *Gymnodinium catenatum* associated with coastal upwelling plumes off central Portugal. *Acta Oecologica*, 24, 125-132.
- Moline, M.A., Claustre, H., Frazer, T.K., Schofield, O., Vernet, M. (2004). Alteration of the food web along the Antarctic Peninsula in response to a regional warming trend. *Global Change Biology*, 10, 1973-1980.
- Nakamura, Y., Suzuki, S., Hiromi, J. (1995). Population dynamics of heterotrophic dinoflagellates during a *Gymnodinium mikimotoi* red tide in the Seto Inland Sea. *Marine Ecology Progress Series*, 125, 269-277.

- Not, F., Latasa, M., Marie, D., Cariou, T., Vaulot, D., Simon, N. (2004). A single species, *Micromonas pusilla* (Prasinophyceae), dominates the Eukaryotic picoplankton in the Western English Channel. *Applied and Environmental Microbiology*, 70, 4064-4072.
- Reynold, C. S. (1988). Functional morphology and the adaptive strategies of freshwater phytoplankton. In: Sandgren, C.D. (ed.), *Growth and Reproductive Strategies of Freshwater Phytoplankton*. Cambridge University Press, pp. 388-433.
- Reynolds, C.S. (1996). Plant file of the Pelagic. *The Proceedings of the International Association of Theoretical and Applied Limnology*, 26, 97-113.
- Reynolds, C.S. (1997). *Vegetative Process in the Pelagic: A model for Ecosystem Theory*. Ecology Institute, Oldendorf/Luhe, Germany.
- Reynolds, C., Huszar, V., Kruk, C., Naselli-Flores, L., Melo, S. (2002). Towards a functional classification of the freshwater phytoplankton. *Journal of Plankton Research*, 24, 417-428.
- Ricard, M. (1987). *Atlas du Phytoplancton Marin. II. Diatomophycées*. Centre National de la Recherche Scientifique. Paris. France.
- Sanderson, J.C., Dring, M.J., Davidson, K., Kelly, M.S. (2012). Culture, yield and bioremediation potential of *Palmaria palmata* (Linnaeus) Weber & Mohr and *Saccharina latissima* (Linnaeus) C.E. Lane, C. Mayes, Druehl & G.W. Sauders adjacent to fish farm cages in northwest Scotland. *Aquaculture*, 354-355, 128-135.
- Schlüter, L., Havskum, H. (1997). Phytoplankton pigments in relation to carbon content in phytoplankton communities. *Marine Ecology Progress Series*, 155, 55-65.
- Schlüter, L., Møhlenberg, F., Havskum, H., Larsen, S. (2000). The use of phytoplankton pigments for identifying and quantifying phytoplankton groups in coastal areas: testing the influence of light and nutrients on pigment/chlorophyll a ratios. *Marine Ecology Progress Series*, 192, 49-63.
- Schmid, H., Bauer, F., Stich, H.B. (1998). Determination of algal biomass with HPLC pigment analysis from lakes of different trophic state in comparison to microscopically measured biomass. *Journal of Plankton Research*, 20, 1651-1661.
- Smayda, T.J. (1957). Phytoplankton studies in Lower Narragansett Bay. *Limnology and Oceanography*, 2, 342-359.
- Smayda, T.J., Boleyn, B.J. (1966). Experimental observations on the flotation of marine diatoms. II. *Skeletonema costatum* and *Rhizosolenia setigera*. *Limnology and Oceanography*, 11, 18-34.
- Smayda, T.J., Reynolds, C.S. (2001). Community assembly in marine phytoplankton: application of recent models to harmful dinoflagellates blooms. *Journal of Plankton Research*, 23, 447-461.
- Smayda, T.J., Reynolds, C.S. (2003). Strategies of marine dinoflagellate survival and some rules of assembly. *Journal of Sea Research*, 49, 95-106.
- Sournia, A. (1986). *Atlas du Phytoplancton Marin. I. Introduction, Cyanophycées, Dictyophycées, Dinophycées et Raphidophycées*. Centre National de la Recherche Scientifique. Paris. France.
- Spector, D. L. (1984). *Dinoflagellates*. Academic Press Inc., New York, London, 545 pp.

- Staats, N., De Winder, B., Stal, L., Mur, L. (1999). Isolation and characterization of extracellular polysaccharides from the epipelagic diatoms *Cylindrotheca closterium* and *Navicula salinarum*. *European Journal of Phycology*, 34, 161-169.
- Tappan, H. (1980). *The Paleobiology of Plant Protists*. W.H. Freeman & Company, San Francisco, 1028pp.
- Tett, P., Edwards, A., Jones, K. (1986). A model for the growth of Shelf-Sea phytoplankton in Summer. *Estuarine, Coastal and Shelf Science*, 23, 641-672.
- Tomas, C. (1997). *Identifying Marine Phytoplankton*, Academic Press, San Diego, 858 pp.
- Tyrrell, T., Merico, A. (2004). *Emiliana huxleyi*: bloom observations and the conditions that induce them. In: Thierstein, H.R., Young, J.R. (eds.) *Coccolithophores: from molecular processes to global impact*. Berlin, Germany, Springer, 75-97.
- Utermöhl, H. (1958). Zur Vervollkommnung der quantitativen Phytoplankton-Methodik. *Mitt. Int. Ver. Limnol.*, 9, 1-38.
- Varella, D.E., Willers, V., Crawford, D.W. (2011). Effect of zinc availability on growth, morphology, and nutrient incorporation in a coastal and an oceanic diatom. *Journal of Phycology*, 47, 302-312.
- Yamamoto, T., Suzuki, M., Kim, K., Asaoka, S. (2012). Growth and uptake kinetics of phosphate by benthic microalga *Nitzschia* sp. Isolated from Hiroshima Bay, Japan. *Phycological Research*, 60, 223-228.
- Yoder, J.A. (1979). A comparison between cell division rate of natural populations of the marine diatom *Skeletonema costatum* (Greville) Cleve grown in dialysis culture and that predicted from a mathematical model. *Limnology and Oceanography*, 24, 97-106.
- Wright, S.W., Ishikawa, A., Marchant, H.J., Davidson, A.T., van den Enden, R.L., Nash, G.V. (2009). Composition and significance of picophytoplankton in Antarctic waters. *Polar Biology*, 32, 797-808.
- Wright, S.W., Jeffrey, S.W. (2006). Pigment markers for phytoplankton production. In: Volkmann J.K. (Ed.), *Marine Organic Matter: Biomarkers, Isotopes and DNA*, Springer-Verlag, Berlin, pp. 71-104.
- Wright, S.W., Thomas, D.P., Marchant, J., Higgins, H.W., Mackey, M.D., Mackey, D.J. (1996). Analysis of phytoplankton of the Australian sector of the Southern Ocean: comparisons of microscopy and size frequency data with interpretations of pigment HPLC data using the 'CHEMTAX' matrix factorisation program. *Marine Ecology Progress Series*, 144, 285-298.
- Zapata, M., Jeffrey, S.W., Wright, S.W., Rodríguez, F., Garrido, J.L., Clementson, L. (2004). Photosynthetic pigments in 37 species (65 strains) of Haptophyta, implications for oceanography and chemotaxonomy. *Marine Ecology Progress Series*, 270, 83-102.
- Zapata, M., Rodríguez, F., Garrido, J.L. (2000). Separation of chlorophylls and carotenoids from marine phytoplankton: a new HPLC method using a reversed phase C8 column and pyridine-containing mobile phases. *Marine Ecology Progress Series*, 195, 29-45.

Tables

Table 1 – Pigment concentrations ($\text{mg}\cdot\text{m}^{-3}$) obtained in this study (average and minimum-maximum values).

Table 2 - Input and output ratios of marker pigments to chlorophyll a for surface and deep chlorophyll maximum (fluorescence) .

Table 3 – Average, minimum and maximum abundance values ($\times 10^3 \text{ cells}\cdot\text{L}^{-1}$) of the seventeen most abundant taxa observed in this study. Each taxon contributed at least 0.15% for the total phytoplankton abundance. Information on the classification used to separate diatoms is also provided (centric vs pennate).

Table 1 – Pigment concentrations ($\text{mg}\cdot\text{m}^{-3}$) obtained in this study (average and minimum-maximum values).

| Abbreviation | Pigment | Average and range of concentrations ($\text{mg}\cdot\text{m}^{-3}$) |
|---|--|---|
| Chl <i>a</i> | Chlorophyll <i>a</i> | 0.971 (0.639 – 2.570) |
| Chlide <i>a</i> | Chlorophyllide <i>a</i> | 0.015 (0.002 – 0.160) |
| Chl <i>b</i> | Chlorophyll <i>b</i> | 0.142 (0.089 – 0.337) |
| Chl <i>c</i> ₁ | Chlorophyll <i>c</i> ₁ | 0.003 (0.000 – 0.031) |
| Chl <i>c</i> ₂ | Chlorophyll <i>c</i> ₂ | 0.119 (0.074 – 0.363) |
| Chl <i>c</i> ₃ | Chlorophyll <i>c</i> ₃ | 0.076 (0.049 – 0.166) |
| Mg DVP | Mg-2,4-divinylpheoporphyrin <i>a</i> ₅ monomethyl ester | 0.012 (0.007 – 0.032) |
| Diadino | Diadinoxanthin | 0.043 (0.023 – 0.152) |
| Dino | Dinoxanthin | 0.004 (0.001 – 0.017) |
| Lut | Lutein | 0.004 (0.002 – 0.013) |
| Diato | Diatoxanthin | 0.006 (0.002 – 0.018) |
| Allo | Alloxanthin | 0.084 (0.047 – 0.278) |
| Zea | Zeaxanthin | 0.009 (0.005 – 0.019) |
| Perid | Peridinin | 0.049 (0.019 – 0.174) |
| Neo | Neoxanthin | 0.013 (0.008 – 0.031) |
| But-fuco | 19'-Butanoyloxyfucoxanthin | 0.005 (0.002 – 0.011) |
| Fuco | Fucoxanthin | 0.270 (0.152 – 0.580) |
| Hex-fuco | 19'-Hexanoyloxyfucoxanthin | 0.086 (0.055 – 0.231) |
| Hex-kfuco | 19'-Hexanoyloxy-4-ketofucoxanthin | 0.024 (0.016 – 0.046) |
| Croco | Crocoxanthin | 0.008 (0.005 – 0.027) |
| Viola | Violaxanthin | 0.017 (0.010 – 0.046) |
| Prasino | Prasinoxanthin | 0.031 (0.019 – 0.069) |
| β,β -Car | β,β -Carotene | 0.024 (0.015 – 0.062) |
| B, ϵ -Car | B, ϵ -Carotene | 0.015 (0.009 – 0.040) |
| Chl <i>c</i> ₂ -MGDG [18:14] | Chl <i>c</i> ₂ -monogalactosyldiacylglyceride ester [18:14] | 0.010 (0.006 – 0.021) |
| Chl <i>c</i> ₂ -MGDG [14:14] | Chl <i>c</i> ₂ -monogalactosyldiacylglyceride ester [14:14] | 0.008 (0.004 – 0.029) |
| Pheide <i>a</i> | Pheophorbide <i>a</i> | 0.024 (0.009 – 0.106) |
| Phe <i>a</i> | Pheophytin <i>a</i> | 0.021 (0.010 – 0.057) |

Table 2 - Input and output ratios of marker pigments to chlorophyll a for surface and deep chlorophyll maximum (fluorescence) .

| Initial ratios | | | | | | | | | | | | | | | | | | |
|---------------------|-----------|-----------|-------|----------|-------|-------|-----------|-------|---------|----------|-------|-------|-------|---------|-------|------------------------|------------------------|---------|
| Taxonomic group | Chl c_3 | Chl c_1 | Perid | But-fuco | Fuco | Neo | Hex-kfuco | Viola | Prasino | Hex-fuco | Dino | Zea | Lut | Chl b | Allo | Chl c_2 -MGDG[18:14] | Chl c_2 -MGDG[14:14] | Chl a |
| Diatoms-1 | 0.000 | 0.107 | 0.000 | 0.000 | 0.675 | 0.000 | 0.000 | 0.000 | 0.000 | 0.000 | 0.000 | 0.000 | 0.000 | 0.000 | 0.000 | 0.000 | 0.000 | 1.000 |
| Dinoflagellates-1 | 0.000 | 0.000 | 0.609 | 0.000 | 0.000 | 0.000 | 0.000 | 0.000 | 0.000 | 0.000 | 0.039 | 0.000 | 0.000 | 0.000 | 0.000 | 0.000 | 0.000 | 1.000 |
| Haptophytes-6 | 0.346 | 0.000 | 0.000 | 0.026 | 0.723 | 0.000 | 0.150 | 0.000 | 0.000 | 0.099 | 0.000 | 0.000 | 0.000 | 0.000 | 0.000 | 0.068 | 0.000 | 1.000 |
| Haptophytes-7 | 0.202 | 0.014 | 0.000 | 0.011 | 0.388 | 0.000 | 0.151 | 0.000 | 0.000 | 0.567 | 0.000 | 0.000 | 0.000 | 0.000 | 0.000 | 0.094 | 0.103 | 1.000 |
| Haptophytes-8 | 0.171 | 0.000 | 0.000 | 0.103 | 0.300 | 0.000 | 0.058 | 0.000 | 0.000 | 0.371 | 0.000 | 0.000 | 0.000 | 0.000 | 0.000 | 0.058 | 0.000 | 1.000 |
| Prasinophytes-3 | 0.000 | 0.000 | 0.000 | 0.000 | 0.000 | 0.093 | 0.000 | 0.035 | 0.222 | 0.000 | 0.000 | 0.057 | 0.011 | 0.911 | 0.000 | 0.000 | 0.000 | 1.000 |
| Cryptophytes | 0.000 | 0.000 | 0.000 | 0.000 | 0.000 | 0.000 | 0.000 | 0.000 | 0.000 | 0.000 | 0.000 | 0.000 | 0.000 | 0.000 | 0.253 | 0.000 | 0.000 | 1.000 |
| Final ratios (Surf) | | | | | | | | | | | | | | | | | | |
| Taxonomic group | Chl c_3 | Chl c_1 | Perid | But-fuco | Fuco | Neo | Hex-kfuco | Viola | Prasino | Hex-fuco | Dino | Zea | Lut | Chl b | Allo | Chl c_2 -MGDG[18:14] | Chl c_2 -MGDG[14:14] | Chl a |
| Diatoms-1 | 0.000 | 0.096 | 0.000 | 0.000 | 0.523 | 0.000 | 0.000 | 0.000 | 0.000 | 0.000 | 0.000 | 0.000 | 0.000 | 0.000 | 0.000 | 0.000 | 0.000 | 1.000 |
| Dinoflagellates-1 | 0.000 | 0.000 | 0.499 | 0.000 | 0.000 | 0.000 | 0.000 | 0.000 | 0.000 | 0.000 | 0.041 | 0.000 | 0.000 | 0.000 | 0.000 | 0.000 | 0.000 | 1.000 |
| Haptophytes-6 | 0.280 | 0.000 | 0.000 | 0.015 | 0.845 | 0.000 | 0.074 | 0.000 | 0.000 | 0.076 | 0.000 | 0.000 | 0.000 | 0.000 | 0.000 | 0.017 | 0.000 | 1.000 |
| Haptophytes-7 | 0.171 | 0.011 | 0.000 | 0.009 | 0.307 | 0.000 | 0.104 | 0.000 | 0.000 | 0.800 | 0.000 | 0.000 | 0.000 | 0.000 | 0.000 | 0.071 | 0.091 | 1.000 |
| Haptophytes-8 | 0.134 | 0.000 | 0.000 | 0.087 | 0.251 | 0.000 | 0.047 | 0.000 | 0.000 | 0.312 | 0.000 | 0.000 | 0.000 | 0.000 | 0.000 | 0.049 | 0.000 | 1.000 |
| Prasinophytes-3 | 0.000 | 0.000 | 0.000 | 0.000 | 0.000 | 0.063 | 0.000 | 0.076 | 0.147 | 0.000 | 0.000 | 0.043 | 0.013 | 0.652 | 0.000 | 0.000 | 0.000 | 1.000 |
| Cryptophytes | 0.000 | 0.000 | 0.000 | 0.000 | 0.000 | 0.000 | 0.000 | 0.000 | 0.000 | 0.000 | 0.000 | 0.000 | 0.000 | 0.000 | 0.258 | 0.000 | 0.000 | 1.000 |
| Final ratios (DCM) | | | | | | | | | | | | | | | | | | |
| Taxonomic group | Chl c_3 | Chl c_1 | Perid | But-fuco | Fuco | Neo | Hex-kfuco | Viola | Prasino | Hex-fuco | Dino | Zea | Lut | Chl b | Allo | Chl c_2 -MGDG[18:14] | Chl c_2 -MGDG[14:14] | Chl a |
| Diatoms-1 | 0.000 | 0.084 | 0.000 | 0.000 | 0.558 | 0.000 | 0.000 | 0.000 | 0.000 | 0.000 | 0.000 | 0.000 | 0.000 | 0.000 | 0.000 | 0.000 | 0.000 | 1.000 |
| Dinoflagellates-1 | 0.000 | 0.000 | 0.466 | 0.000 | 0.000 | 0.000 | 0.000 | 0.000 | 0.000 | 0.000 | 0.036 | 0.000 | 0.000 | 0.000 | 0.000 | 0.000 | 0.000 | 1.000 |
| Haptophytes-6 | 0.312 | 0.000 | 0.000 | 0.008 | 0.902 | 0.000 | 0.089 | 0.000 | 0.000 | 0.083 | 0.000 | 0.000 | 0.000 | 0.000 | 0.000 | 0.018 | 0.000 | 1.000 |
| Haptophytes-7 | 0.172 | 0.010 | 0.000 | 0.010 | 0.326 | 0.000 | 0.131 | 0.000 | 0.000 | 0.731 | 0.000 | 0.000 | 0.000 | 0.000 | 0.000 | 0.068 | 0.094 | 1.000 |
| Haptophytes-8 | 0.142 | 0.000 | 0.000 | 0.086 | 0.240 | 0.000 | 0.037 | 0.000 | 0.000 | 0.320 | 0.000 | 0.000 | 0.000 | 0.000 | 0.000 | 0.048 | 0.000 | 1.000 |
| Prasinophytes-3 | 0.000 | 0.000 | 0.000 | 0.000 | 0.000 | 0.067 | 0.000 | 0.060 | 0.160 | 0.000 | 0.000 | 0.041 | 0.010 | 0.679 | 0.000 | 0.000 | 0.000 | 1.000 |
| Cryptophytes | 0.000 | 0.000 | 0.000 | 0.000 | 0.000 | 0.000 | 0.000 | 0.000 | 0.000 | 0.000 | 0.000 | 0.000 | 0.000 | 0.000 | 0.231 | 0.000 | 0.000 | 1.000 |

Table 3 – Average, minimum and maximum abundance values ($\times 10^3$ cells.L⁻¹) of the seventeen most abundant taxa observed in this study. Each taxon contributed at least 0.15% for the total phytoplankton abundance. Information on the classification used to separate diatoms is also provided (centric vs pennate).

| Genera | Abundances ($\times 10^3$ cells.L ⁻¹) | | Diatom typology |
|--------------------------|---|---------------|--------------------|
| | Average | (min-max) | |
| Bacillariophyceae | | | |
| <i>Chaetoceros</i> | 460.0 | 0.0 – 8100 | Centric |
| <i>Dactyliosolen</i> | 64.8 | 0.0 – 240 | Centric |
| <i>Detonula</i> | 97.9 | 0.0 – 2680 | Centric |
| <i>Guinardia</i> | 41.4 | 0.0 – 410 | Centric |
| <i>Leptocylindrus</i> | 43.6 | 0.0 – 630 | Centric |
| <i>Paralia</i> | 363.6 | 0.0 – 1230 | Centric |
| <i>Rhizosolenia</i> | 124.1 | 0.0 – 820 | Centric |
| <i>Skeletonema</i> | 5998.1 | 0.0 – 99440 | Centric |
| <i>Cylindrotheca</i> | 1139.5 | 300.0 – 2380 | Pennate |
| <i>Navicula</i> | 35.0 | 0.0 – 240 | Pennate |
| <i>Nitzschia</i> | 186.2 | 20.0 – 980 | Pennate |
| Dinophyceae | | | |
| <i>Amphidinium</i> | 77.14 | 0.0 – 220 | - |
| Gymnodinioid | 12046.2 | 570.0 – 57930 | - |
| <i>Heterocapsa</i> | 53.6 | 0.0 – 1360 | - |
| <i>Katodinium</i> | 342.1 | 80.0 – 790 | - |
| <i>Prorocentrum</i> | 103.1 | 20.0 – 300 | - |
| <i>Scropsiella</i> | 176.4 | 0.0 – 880 | - |